Human hepatocyte-targeted cytoplasmic delivery of siRNA using bio-nanocapsule-liposome complexes

バイオナノカプセル-リポソーム複合体による

ヒト肝臓細胞特異的細胞質内 siRNA 送達法の開発

Masaharu SOMIYA

曽宮 正晴

March, 2016

Table of contents

Chapter I General introduction

1.1. Drug delivery system (DDS)

Drug delivery system (DDS) has been considered as a key technology to achieve efficient drug treatment by reducing undesirable side effects [1–3]. Especially, the highly cytotoxic drugs, such as anti-cancer drugs, should be delivered to the diseased site specifically to maximize the therapeutics effect. As DDS carriers, various types of nano-sized materials, namely, nanocarriers are used [4]. When drugs are encapsulated into nanocarriers, the side effect of drugs could be reduced due to the reduction of nonspecific diffusion of drug to healthy tissues. Furthermore, the blood clearance time of encapsulated drug becomes longer, since nanocarriers (generally ~100-nm diameter) could evade renal filtration that excretes nanoparticles of less than 6-nm dimeter [5].

Nanocarrier-based drugs (nanomedicines) have been clinically available as mainly anti-cancer drugs from 1995. Since tumor tissues show leaky blood vessel structure and impaired lymphatic drainage, nanomedicines can be accumulated into tumor tissues (enhanced permeability and retention (EPR) effect) [6,7]. Based on this phenomenon, nanomedicines are recognized as an effective strategy for cancer treatment. Doxil, a structurally stabilized liposomal doxorubicin, is the most successful nanomedicine and has been used clinically for cancer treatment from 1995 [8]. Doxil is ~100-nm spherical liposome encapsulating doxorubicin in its inner space and displaying polyethylene glycol (PEG) chain. Doxil shows longer circulation time in blood and significantly less side-effect than free doxorubicin. Currently, nanomicelles composed of block copolymer have emerged and used for the delivery of anti-cancer drugs such as paclitaxel, doxorubicin, and cisplatin, etc. [9] Several ongoing clinical trials showed excellent efficacy of nanomicelles-mediated drug delivery. Thus, nanomedicine is a promising formulation of anti-cancer drugs in terms of the tumor-directed DDS.

Contrary to the tumor targeting based on the EPR effect (*i.e.* passive targeting), it has been still difficult to achieve the active targeting to the specific tissues other than tumor tissues. Several ligands that can recognize the specific membrane proteins of interest have been used to modify the surface of nanoparticles, however, this strategy has not fully approved for clinically available formulation, due to the difficulties of the selection of target molecule that is expressed specifically in target site and not in non-target sites.

1.2. Bio-nanocapsule (BNC) as a hepatitis B virus-mimicking DDS nanocarrier

Although nanocarriers should be implemented with targeting machinery, active targeting has not been achieved yet, since the nanofabrication of functional components into the tiny particle is difficult (*i.e.*, a spatial limitation of synthetic nanocarriers). On the other hand, viruses are natural

occurring nanocarriers [10], of which the diameter is from several tens to hundreds of nanometers. They could infect host cells efficiently and specifically by the rational assembly of their components (surface proteins, lipid bilayer, and core proteins). Several functions of viruses are shared with nanocarriers as follows; 1) the evading activity from host immune systems (stealth activity), 2) the targeting activity to specific cells (host tropism), 3) the cell entry activity, 4) the controlled release activity of their genetic materials, and 5) the transporting activity of their contents to appropriate organelles. Indeed, some viruses are used as gene vectors from basic to clinical research [11]. They show incredible transfection efficiency compared with conventional synthetic vectors such as cationic liposomes [12,13], illustrating the excellent potentials of virus-derived DDS nanocarriers. Similarly, virus-like particles (VLPs) are used as a DDS nanocarrier [14–16]. VLPs are composed of viral proteins (capsid or envelope protein) with or without lipid bilayer. When drugs are incorporated into VLPs, they could be delivered to the host cells of original virus. Since VLPs lack viral genome, they could not replicate and thereby be used as safe DDS nanocarrier. Although viral vectors and VLPs thus possess advantages as DDS nanocarrier, the following issues should be addressed before moving to the clinical application. First, large scale production system of virus-derived nanocarriers has to be established; and second, immunogenicity of viral proteins should be eliminated.

Hepatitis B virus (HBV, Fig. 1.1 left) has three types of surface antigens (small (S) protein containing S region, middle (M) protein containing pre-S2 + S regions, and large (L) protein containing pre-S1 + pre-S2 + S regions) [17]. Due to the inhibitory effect of pre-S1 region on the secretory apparatus, the synthesis of L protein had been failed for long time. By the addition of synthetic signal peptide at the N-terminus of L protein, Kuroda *et al.* succeeded in the production of large amounts of HBV envelope L protein particle using recombinant yeast cells in 1992 [18]. One recombinant L particle displays about 110 molecules of L protein embedded in lipid bilayer derived from yeast endoplasmic reticulum. Initially, the VLP is recognized as an immunogen of HBV vaccine for inducing effective immune reaction against HBV. Particularly, the pre-S1 region of L protein is involved in the recognition with the HBV receptor on the surface of human hepatocyte [19,20]. Thereafter, recombinant L particle expected to behave like HBV in terms of human hepatocyte-specific infection. After the introduction of plasmid DNA or compounds into the inner hollow space of L particle by electroporation, they could be delivered to human hepatocyte *in vitro* and *in vivo* [21]. This nanoparticle was designated as “bio-nanocapsule (BNC)” (Fig. 1.1 right) and several types of BNC derivatives have been developed so far [22].

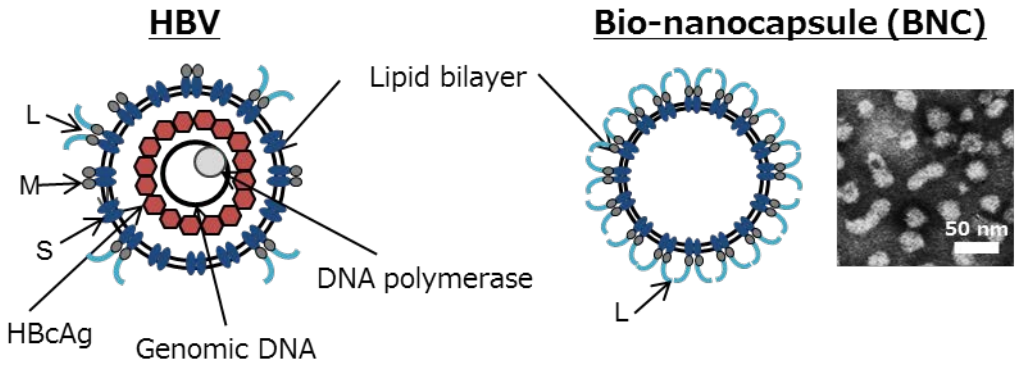

Fig. 1.1 Schematic representations of HBV and BNC. HBV is composed of envelope (lipid bilayer and surface proteins [S, M, and L protein]) and their contents (genomic DNA, core proteins [HBcAg], and DNA polymerase). BNC is composed of lipid bilayer and L protein. BNCs are spherical ~100-nm nanoparticles (from transmission electron microscope observation).

The most feasible formulation of BNC is the liposomal complex. When BNCs are mixed with liposomes (LPs), BNC spontaneously form stable BNC-LP complex [23]. Since various methods to encapsulate payloads into LPs have been already established, the availability of BNC-LP complex could expand the possibility of BNC technology in various applications. Currently, after the optimization of complex formation between BNC and LPs, BNC was found to form “virosome”, defined as a hybrid of viral proteins and LP [24,25]. The lipid bilayer of BNC fully fuses with LP membrane under acidic condition at high temperature. Virosome formulation enables us to control both lipid composition and BNC contents of BNC-LP complex. However, one question arises; how BNC fuses with lipid membrane? I presumed that BNC harbors membrane fusion activity, and thereby mediates the fusion between BNC and cellular membrane for the entry into cytoplasm. This activity might play a pivotal role in the uncoating process of HBV. In Chapter II, I demonstrated the identification of membrane fusion activity of BNC, the delineation of fusogenic domain in pre-S1 region, and the elucidation of intracellular trafficking of BNC-LP complexes.

1.3. Short interfering RNA (siRNA) therapeutics: potentials and problems

RNA interference (RNAi) has been recognized as a novel therapeutic strategy [26–28]. RNAi-mediated gene silencing could be an effective treatment for incurable diseases, since it mediates the disease pathogenesis directly. RNAi-based therapeutics including short interfering RNA (siRNA) and micro RNA (miRNA) are recently investigated against various target genes. Especially, siRNA can target and suppress gene of interest specifically after the incorporation into RNA-induced silencing complex (RISC) [29]. Whereas such nucleic acid medicines have been recognized as next generation drug, there has been no commercial RNAi-based drug to date. The most important issue

regarding clinical application of RNAi therapeutics is the difficulties of *in vivo* nucleic acids delivery. Since nucleic acid medicines are highly hydrophilic and large molecules (ca. siRNA, ~13 kDa), they are hard to penetrate cellular membrane by themselves. Furthermore, RNAi-based drugs must be delivered to the cytoplasm of target cells where RISC functions to silence target gene. Therefore, nucleic acid medicines had to be delivered intracellularly by DDS [30].

Several types of nanocarriers have been developed and evaluated so far [31]. Most successful nanocarrier for siRNA is lipid nanoparticle (LNP) [32,33]. The LNP is composed of pH-sensitive lipid, helper lipid, PEGylated lipid, and siRNA. Generally, LNPs show 50~100-nm in diameter and charge neutrally, which are suitable for intravenous administration. Particularly, pH-sensitive lipid, namely ionizable lipid, is the most important component as it possesses two following functions; the encapsulation of siRNA into LNP *via* electrostatic interaction between cationic ionizable lipid and anionic siRNA at acidic pH, and the induction of lipid mixing in the acidic endosome/lysosome after the internalization into cell *via* endocytosis, followed by the endosomal escape of siRNA. Furthermore, LNP could bind to apolipoprotein in blood, and accumulate to liver cells specifically by the interaction with apolipoprotein receptor on the hepatocytes [34]. Due to the rational design as mentioned above, LNP could deliver siRNA to hepatocyte efficiently, and subsequently induce gene silencing effectively even in the low-dose administration [35]. LNP formulation shows good tolerability in the clinical trials, whereas either immunological reaction or infusion-related toxicity is still observed [28]. These side-effects are probably due to the immunogenicity of siRNA and LNP. Moreover, cationic nature of the ionizable lipid in acidic endosome/lysosome is not suitable for the efficient release of siRNA, since the electrostatic interaction between ionizable lipid and siRNA could prevent the release of siRNA from LNP. Thus, nanocarriers excluding cationic and cytotoxic materials have been expected as safer than LNP for the forthcoming siRNA therapeutics. In Chapter III, I demonstrated the establishment of novel encapsulation method of siRNA into non-cationic LPs, and the targeted siRNA delivery by BNC-LP complexes to human hepatic cells *in vitro*.

1.4. References

[1] R. Langer, Drug delivery and targeting, Nature. 392 (1998) 5–10. doi:10.1517/14728222.2.1.145.

[2] T. Lammers, F. Kiessling, W.E. Hennink, G. Storm, Drug targeting to tumors: Principles, pitfalls and (pre-) clinical progress, J. Control. Release. 161 (2012) 175–187. doi:10.1016/j.jconrel.2011.09.063.

[3] L. Brannon-Peppas, J.O. Blanchette, Nanoparticle and targeted systems for cancer therapy, Adv. Drug Deliv. Rev. 64 (2012) 206–212. doi:10.1016/j.addr.2012.09.033.

[4] D. Peer, J.M. Karp, S. Hong, O.C. Farokhzad, R. Margalit, R. Langer, Nanocarriers as an emerging platform for cancer therapy., Nat. Nanotechnol. 2 (2007) 751–760. doi:10.1038/nnano.2007.387.

[5] H. Soo Choi, W. Liu, P. Misra, E. Tanaka, J.P. Zimmer, B. Itty Ipe, et al., Renal clearance of quantum dots, Nat. Biotechnol. 25 (2007) 1165–1170. doi:10.1038/nbt1340.

[6] Y. Matsumura, H. Maeda, A new concept for macromolecular therapeutics in cnacer chemotherapy: mechanism of tumoritropic accumulatio of proteins and the antitumor agents Smancs, Cancer Res. 46 (1986) 6387– 6392. http://cancerres.aacrjournals.org/content/46/12_Part_1/6387.short (accessed January 22, 2015).

[7] H. Maeda, Toward a full understanding of the EPR effect in primary and metastatic tumors as well as issues related to its heterogeneity, Adv. Drug Deliv. Rev. (2015) 2–5. doi:10.1016/j.addr.2015.01.002.

[8] Y. Barenholz, Doxil - The first FDA-approved nano-drug: Lessons learned, J. Control. Release. 160 (2012) 117–134. doi:10.1016/j.jconrel.2012.03.020.

[9] H. Cabral, K. Kataoka, Progress of drug-loaded polymeric micelles into clinical studies, J. Control. Release. 190 (2014) 465–476. doi:10.1016/j.jconrel.2014.06.042.

[10] Y. Seow, M.J. Wood, Biological gene delivery vehicles: beyond viral vectors., Mol. Ther. 17 (2009) 767–77. doi:10.1038/mt.2009.41.

[11] N.A. Kootstra, I.M. Verma, Gene therapy with viral vectors., Annu. Rev. Pharmacol. Toxicol. 43 (2003) 413–39. doi:10.1146/annurev.pharmtox.43.100901.140257.

[12] S. Hama, H. Akita, R. Ito, H. Mizuguchi, T. Hayakawa, H. Harashima, Quantitative comparison of intracellular trafficking and nuclear transcription between adenoviral and lipoplex systems., Mol. Ther. 13 (2006) 786–94. doi:10.1016/j.ymthe.2005.10.007.

[13] S. Hama, H. Akita, S. Iida, H. Mizuguchi, H. Harashima, Quantitative and mechanism-based investigation of post-nuclear delivery events between adenovirus and lipoplex., Nucleic Acids Res. 35 (2007) 1533–43. doi:10.1093/nar/gkl1165.

[14] A. Touze, P. Coursaget, In vitro gene transfer using human papillomavirus-like particles, Nucleic Acids Res. 26 (1998) 1317–1323. doi:10.1093/nar/26.5.1317.

[15] T. Inoue, M.A. Kawano, R.U. Takahashi, H. Tsukamoto, T. Enomoto, T. Imai, et al., Engineering of SV40-based nano-capsules for delivery of heterologous proteins as fusions with the minor capsid proteins VP2/3, J. Biotechnol. 134 (2008) 181–192. doi:10.1016/j.jbiotec.2007.12.006.

[16] N.G. Cortes-Perez, C. Sapin, L. Jaffrelo, S. Daou, J.P. Grill, P. Langella, et al., Rotavirus-like particles: a novel nanocarrier for the gut., J. Biomed. Biotechnol. 2010 (2010) 317545. doi:10.1155/2010/317545.

[17] P. Tiollais, C. Pourcel, A. Dejean, The hepatitis B virus, Nature. 317 (1985) 489–495. doi:10.1038/317489a0.

[18] S. Kuroda, S. Otaka, T. Miyazaki, M. Nakao, Y. Fujisawa, Hepatitis B virus envelope L protein particles: Synthesis and assembly in Saccharomyces cerevisiae, purification and characterization, J. Biol. Chem. 267 (1992) 1953–1961. http://www.ncbi.nlm.nih.gov/pubmed/18434744.

[19] A.R. Neurath, S.B. Kent, N. Strick, K. Parker, Identification and chemical synthesis of a host cell receptor binding site on hepatitis B virus., Cell. 46 (1986) 429–436. doi:0092-8674(86)90663-X.

[20] P. Gripon, I. Cannie, S. Urban, Efficient Inhibition of Hepatitis B Virus Infection by Acylated Peptides Derived from the Large Viral Surface Protein Efficient Inhibition of Hepatitis B Virus Infection by Acylated Peptides Derived from the Large Viral Surface Protein, J. Virol. 79 (2005) 1613–1622. doi:10.1128/JVI.79.3.1613.

[21] T. Yamada, Y. Iwasaki, H. Tada, H. Iwabuki, M.K.L. Chuah, T. VandenDriessche, et al., Nanoparticles for the delivery of genes and drugs to human hepatocytes., Nat. Biotechnol. 21 (2003) 885–890. doi:10.1038/nbt843.

[22] M. Somiya, S. Kuroda, Development of a Virus-mimicking Nanocarrier for Drug Delivery Systems: the Bio-nanocapsule., Adv. Drug Deliv. Rev. (2015). doi:10.1016/j.addr.2015.10.003.

[23] J. Jung, T. Matsuzaki, K. Tatematsu, T. Okajima, K. Tanizawa, S. Kuroda, Bio-nanocapsule conjugated with liposomes for in vivo pinpoint delivery of various materials., J. Control. Release. 126 (2008) 255–64. doi:10.1016/j.jconrel.2007.12.002.

[24] D. Felnerova, J.F. Viret, R. Glück, C. Moser, Liposomes and virosomes as delivery systems for antigens, nucleic acids and drugs, Curr. Opin. Biotechnol. 15 (2004) 518–529. doi:10.1016/j.copbio.2004.10.005.

[25] Q. Liu, J. Jung, M. Somiya, M. Iijima, D. Andrés, K. Choi, Virosomes of hepatitis B virus envelope L proteins containing doxorubicin : synergistic enhancement of human liver-specific antitumor growth activity by radiotherapy, Int. J. Nanomedicine. 10 (2015) 4159–4172. doi:10.2147/IJN.S84295.

[26] A. de Fougerolles, H. Vornlocher, J. Maraganore, J. Lieberman, Interfering with disease: a progress report on siRNA-based therapeutics., Nat. Rev. Drug Discov. 6 (2007) 443–453. doi:10.1038/nrd2310.

[27] M.R. Lares, J.J. Rossi, D.L. Ouellet, RNAi and small interfering RNAs in human disease therapeutic applications., Trends Biotechnol. 28 (2010) 570–9. doi:10.1016/j.tibtech.2010.07.009.

[28] A. Wittrup, J. Lieberman, Knocking down disease: a progress report on siRNA therapeutics, Nat. Rev. Genet. 16 (2015) 543–552. doi:10.1038/nrg3978.

[29] G. Meister, T. Tuschl, Mechanisms of gene silencing by double-stranded RNA., Nature. 431 (2004) 343–9. doi:10.1038/nature02873.

[30] M. Dominska, D.M. Dykxhoorn, Breaking down the barriers: siRNA delivery and endosome escape., J. Cell Sci. 123 (2010) 1183–9. doi:10.1242/jcs.066399.

[31] R. Kanasty, J.R. Dorkin, A. Vegas, D. Anderson, Delivery materials for siRNA therapeutics., Nat. Mater. 12 (2013) 967–77. doi:10.1038/nmat3765.

[32] Y.Y.C. Tam, S. Chen, P.R. Cullis, Advances in Lipid Nanoparticles for siRNA Delivery., Pharmaceutics. 5 (2013) 498–507. doi:10.3390/pharmaceutics5030498.

[33] C. Wan, T.M. Allen, P.R. Cullis, Lipid nanoparticle delivery systems for siRNA-based therapeutics, Drug Deliv. Transl. Res. 4 (2013) 74–83. doi:10.1007/s13346-013-0161-z.

[34] A. Akinc, W. Querbes, S. De, J. Qin, M. Frank-Kamenetsky, K.N. Jayaprakash, et al., Targeted delivery of RNAi therapeutics with endogenous and exogenous ligand-based mechanisms., Mol. Ther. 18 (2010) 1357–64. doi:10.1038/mt.2010.85.

[35] T. Coelho, D. Adams, A. Silva, P. Lozeron, P.N. Hawkins, T. Mant, et al., Safety and efficacy of RNAi therapy for transthyretin amyloidosis., N. Engl. J. Med. 369 (2013) 819–29. doi:10.1056/NEJMoa1208760.

Chapter II Intracellular Trafficking of Bio-nanocapsule-liposome Complex: Identification of Fusogenic Activity in the Pre-S1 Region of Hepatitis B Virus Surface Antigen L Protein

2.1. Introduction

Hepatitis B virus (HBV) specifically infects the human liver via the action of the HBV surface antigen (HBsAg) L protein, of which the N-terminal half of the pre-S1 region functions as a human hepatocyte-recognition domain [1] In 1992, our group succeeded in overexpressing ~100-nm HBsAg L particles in yeast cells [2]. The L particle contains about 110 molecules of HBsAg L proteins embedded in a unilamellar liposome (LP) derived from yeast endoplasmic reticulum membrane [3]. The similarity of the outside of the HBsAg L particle to that of HBV led us to postulate that L particles would retain the early HBV infection mechanism. Indeed, the L particle has recently been shown to utilize the HBV receptors localized on human liver cells and to enter into these cells through either clathrin-dependent endocytosis or macropinocytosis at the same rate as HBV [4]. After having genes and drugs loaded into their cavity by electroporation, these L particles could deliver their payload specifically to human hepatic cells *in vitro* and *in vivo* with high transfection efficiency [5]. Systemic injection of the L particles containing *HSV-tk* (the herpes simplex virus thymidine kinase gene), followed by the administration of ganciclovir, inhibited the growth of human hepatic tumor in a mouse xenograft model [6]. This versatile L particle, a virosome [7], was designated as a bio-nanocapsule (BNC) [5].

As for the methods used for incorporation of molecules into these BNCs, electroporation often induced unexpected fusion of BNCs, and is therefore unsuitable for good manufacturing protocol (GMP)-based drug production. In 2008, Jung *et al.* found that BNCs could form a stable complex with LPs, facilitating the incorporation of various therapeutic materials (*e.g.*, >45-kb plasmid, 100-nm polystyrene beads) into the BNCs [8]. The BNC–LP complexes could deliver the incorporated materials to the specific site *in vitro* and *in vivo* with the same efficiency as BNCs alone. Since abandonment of electroporation allowed greater control over the manufacturing protocol, these BNC–LP complexes have been recognized as a second-generation BNC technology.

In this study, in order to clarify the mechanism of complex formation between BNCs and LPs, I have examined whether BNCs have fusogenic activity using a lipid-mixing assay. By using fluorescence and electron microscopy, I found that BNC–LP complexes could bind to human hepatic cells and enter into cells via clathrin-mediated endocytosis. Furthermore, our results strongly suggested that BNC–LP complexes release their payloads into the cytoplasm due to the fusogenic activity of the pre-S1 region of the L protein.

2.2. Materials and Methods

2.2.1. Materials

BNCs were prepared from *Saccharomyces cerevisiae* AH22R$^-$ cells harboring the HBsAg L protein-expression plasmid pGLDLIIP39-RcT, as described previously [2,9] Protein concentrations were determined with a BCA protein assay kit (Pierce; Rockford, IL, USA) using bovine serum albumin (BSA; Wako; Osaka, Japan) as a standard. Trypsinized BNCs were prepared as described previously [2]. Monoclonal antibodies against each region of HBsAg L protein (the pre-S1 region, pre-S2 region, and S region) were purchased from the Institute of Immunology (Tokyo, Japan). *p*-Xylene-bis(N-pyridinium bromide) (DPX), pyranine, doxorubicin hydrochloride (DOX), chlorpromazine and amiloride were purchased from Sigma–Aldrich (St. Louis, MO, USA).

2.2.2. Physicochemical analyses

The sizes and ζ-potentials of BNCs were measured in phosphate-buffered saline (PBS) and water, respectively, at 25°C using a Zetasizer Nano ZS system (Malvern; Worcestershire, UK). The amount of IgG bound to BNC was determined at 25°C using a quartz crystal microbalance (QCM), model Twin-Q (As One; Osaka, Japan); a frequency change of 1 Hz corresponds to a weight change of 0.6 ng/cm^2 on the sensor chip [10].

2.2.3. Lipid-mixing assay

Probe LPs (10 μg) containing phosphatidylcholine (PC; Avanti Polar Lipids; Alabaster, AL, USA),
N-(7-nitrobenz-2-oxa-1,3-diazol-4-yl)-1,2-dihexadecanoyl-*sn*-glycero-3-phosphoethanolamine (NBD-PE; Life Technologies; Carlsbad, CA, USA), and Lissamine Rhodamine B 1,2-dihexadecanoyl-*sn*-glycero- 3-phosphoethanolamine, triethylammonium salt (Rh-DHPE; Life Technologies) at a molar ratio of 94:4:2 were mixed with non-probe LPs (40 μg) in 200 μl of PBS. The initial NBD-derived fluorescence (excitation at 470 nm, emission at 540 nm) was monitored at 25 °C for 2 min. After addition of BNCs, PEG4000 (Polysciences; Warrington, PA, USA), Sendai virus (Hayashibara; Okayama, Japan), His6-tagged HIV-TAT peptide (GRKKRRQRRRPPQ; Invitrogen; Carlsbad, CA, USA), or synthetic peptide-displaying LPs (*see below*), the NBD-derived fluorescence was monitored for 30 min. Finally, Triton X-100 was added at 1.0% (v/v, final concentration) to quench the fluorescence resonance energy transfer (FRET) effect completely. In order to generate the synthetic peptide-displaying LPs, HBV pre-S1-derived peptides (Fig. 3A) were synthesized in an N-terminally His6-fused form, and were then displayed onto non-labeled LPs containing 1, 2-dioleoyl-*sn*-glycero-3-{[*N*(5-amino-1-carboxypentyl) iminodiacetic acid]succinyl}, nickel salt (DOGS-NTA-Ni; NOF, Tokyo, Japan). The N-terminally His6-fused HIV-TAT peptide

was used as a positive control. The percentage of NBD-derived fluorescence was calculated as follows: $\%F = (F_{NBD} - F_0) / (F_{100} - F_0)$, where F_0 is the initial NBD-derived fluorescence before the addition of samples; F_{NBD} is the NBD-derived fluorescence at any period after the addition of samples; and F_{100} is the NBD-derived fluorescence after the addition of Triton X-100.

2.2.4. BNC–LP complexes

LPs for the BNC–LP complexes were prepared by using the mixture of 1,2-dipalmitoyl-*sn*-glycero- 3-phosphocholine (DPPC; NOF), 1,2-dipalmitoyl-*sn*-glycero-3-phosphoethanolamine (DPPE; NOF), 1,2-dipalmitoyl-*sn*-glycero-3-phosphoglycerol, sodium salt (DPPG-Na; NOF), and cholesterol (Sigma–Aldrich) at a molar ratio of 15:15:30:40. LPs incorporating nanobeads were prepared by hydrating a lipid film with distilled water containing yellow-green FluoSpheres (20-nm diameter, Life Technologies). In order to label the LP membranes, 1% (mol/mol) of DPPE was replaced with Rh-DHPE. LPs incorporating 8-nm Au nanoparticles (Winered Chemical Corporation; Tokyo, Japan) were purchased from Katayama Chemical Industries (Osaka, Japan). In order to label BNCs, fluorophore was introduced into L proteins using CF488A succinimidyl ester (Biotium; Hayward, CA, USA). BNCs and LPs were mixed at a ratio of 1:20 (w/w) and incubated in Britton Robinson buffer (pH 4.0) [11] at 60 °C for 90 min. The BNC–LP complexes were purified using a 5–40% (w/v) CsCl gradient in isopycnic ultracentrifugation in a P40ST rotor (Hitachi; Tokyo, Japan), at 24,000 rpm at 25 °C for 16 h, followed by overnight dialysis against PBS at 4°C. The diameter of BNC–LP complex was reduced to less than 200 nm by sonication with a probe-type oscillator (Astrason model XL2020; output 20%, 20 kHz, Misonix; Farmingdale, NY, USA) at room temperature.

DOX was encapsulated into BNC–LP complexes by remote loading method as described previously [12]. To measure the amount of leaked DOX, the BNC–LP–DOX complex was incubated with or without LPs composed of 1,2-dioleoyl-*sn*-glycero- 3-phosphocholine (DOPC; NOF) in indicated pH at 37 °C for 30 min. After incubation, the amount of leaked DOX was calculated by the DOX-derived fluorescence (excitation at 488 nm, emission at 590 nm) as described previously [13].

2.2.5. Fluorescence imaging

Human hepatocellular carcinoma cell lines (Huh7 and HepG2), a murine hepatocellular carcinoma cell line (MH1C1), human colon cancer cell line (WiDr), and transformed African green monkey kidney cell line (COS-1) were obtained from the Riken Cell Bank (Tsukuba, Japan). Cells were cultured in Dulbecco's modified Eagle's medium supplemented with 10% fetal bovine serum, at 37 °C under humidified conditions and in 5% (v/v) CO_2. About 10^4 cells, cultured in an 8-well glass-bottomed chamber (Thermo Fisher Scientific; Waltham, MA, USA), were incubated with BNC–LP complexes (5 μg/ml as BNC) at 37°C for the indicated periods, washed with PBS, fixed

with 4% (w/v) paraformaldehyde, and then stained with Hoechst 33342 (Dojindo; Kumamoto, Japan). Fluorescence images were acquired as stacked images (0.5–1.0-μm thickness; 10–15 stacks) using a confocal laser-scanning microscope (FV1000D; Olympus; Tokyo, Japan) and analyzed with ImageJ software (NIH, version 1.47g; Bethesda, MD, USA). Fluorescence intensities were calculated using the following formula: (fluorescence intensity/cell) = Σ (intensity of each dot)/(number of nuclei).

For the colocalization experiments, about 2.0×10^5 cells, cultured in a 35-mm dish, were incubated with BNC–LP–beads complexes (5 μg/ml as BNC) for 30 min, washed with PBS, and further incubated in fresh medium for 0, 5, and 23 h. Cells were incubated in medium containing 100 nM Lysotracker Red (Life Technologies) for 30 min, washed with PBS, and then incubated with 0.025% (w/v) trypsin (Nacalai Tesque; Kyoto, Japan) at 37 °C for 5 min. This was followed by fixation, nuclear staining, and acquisition of fluorescence images. The rates of lysosomal colocalization were calculated using the following formula: (number of dots colocalized with Lysotracker)/(total dots) × 100 (%). The value was obtained from at least 4 independent experiments.

2.2.6. Membrane disruption assay

LPs (DPPC:DPPE: DPPG-Na:choresterol = 15:15:30:40) containing 50 mM DPX and 35 mM pyranine were incubated with BNCs or BNC-LP complexes at indicated pH conditions at 37ºC for 30 min. As described previously [14], the membrane disruption was monitored with the pyranine-derived fluorescence (excitation at 416 nm, emission at 512 nm). The percentage of pyranine was calculated as follows: %leak = $(F_{pyranine} - F_0) / (F_{100} - F_0)$, where F_0 is the initial pyranine-derive fluorescence; $F_{pyranine}$ is the pyranine-derived fluorescence after the 30-min incubation with each samples; and F_{100} is the pyranine-derived fluorescence after the addition of Triton X-100.

2.2.7. Transmission electron microscopy (TEM) imaging

Huh7 cells (about 2.0×10^5 cells), cultured in a 35-mm dish, were incubated with BNC–LP complexes (5 μg/ml as BNC) at 37 °C for 26 h, washed with PBS, fixed with 2% paraformaldehyde and 2% (v/v) glutaraldehyde (GA) at 4°C for 30 min, then fixed with 2% GA at 4 °C overnight, and subsequently postfixed with 2% (w/v) osmium tetroxide for 1 h. Samples were then dehydrated with ethanol, embedded in a resin (Quetol-812, Nisshin EM; Tokyo, Japan), sectioned at 70-nm thickness, and mounted on cupper grids. Sections were then stained with 2% (w/v) uranyl acetate at room temperature for 15 min, washed with distilled water, stained with lead(II) citrate trihydrate (Sigma–Aldrich), and then observed by TEM, using a EM-1400Plus microscope (JEOL; Tokyo, Japan).

2.3. Results and discussion

2.3.1. Fusogenic activity of BNC

The fusogenic activity of BNC was examined using a lipid-mixing assay, utilizing FRET from NBD-PE to Rh-PE, both of which had been incorporated into probe LPs (donor LPs) at quenching concentrations [15]. As shown in Fig. 2.1A, the addition of BNCs to the mixture of probe LPs and non-probe LPs (1:4, w/w) gradually increased the NBD-derived fluorescence, as compared with that observed with addition of PEG4000 and Sendai virus, which have strong fusogenic activity [16–18]. The trypsinized BNCs which lack the N-terminal 125 amino acid (aa) residues [2] (Figs. 2.1B and C) showed no increase in NBD-derived fluorescence (Fig. 2.1D), indicating that at least the N-terminal 125 aa residues of the HBsAg L protein are essential for the fusogenic activity of BNCs.

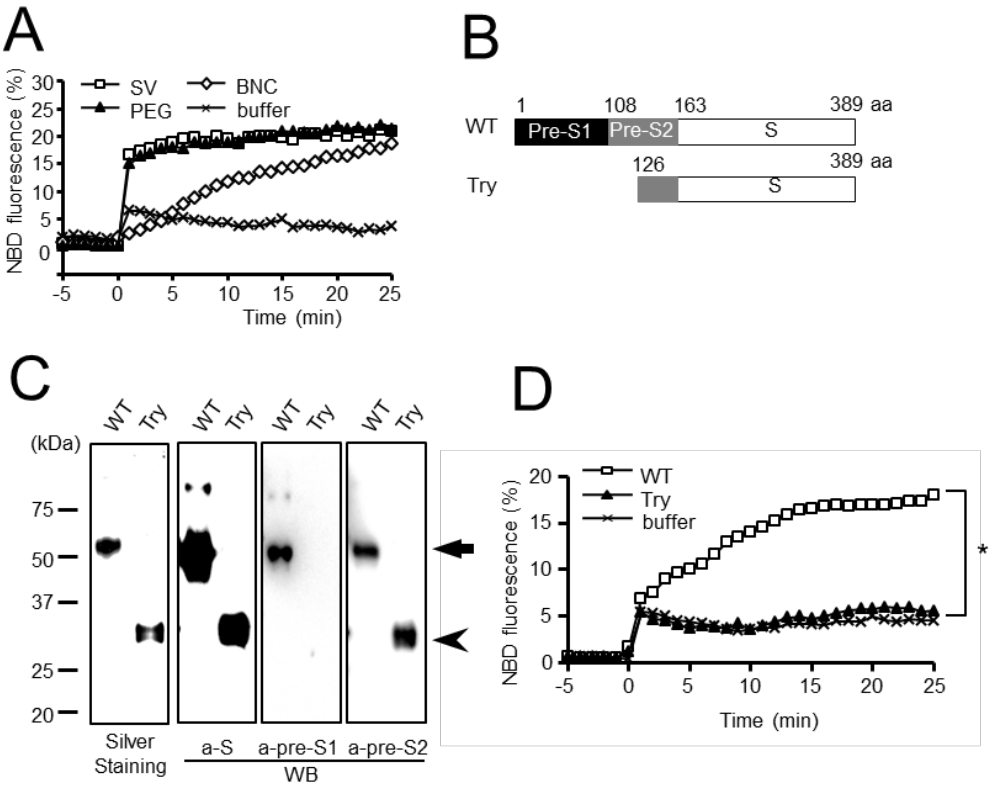

Fig. 2.1 Fusogenic activity of BNCs. *A*, Typical fusion kinetics induced by BNCs (4 μg), Sendai virus (0.9×10^2 hemagglutinating activity), and PEG (final concentration: 8%, w/v). *B*, Schema of full-length (WT) and trypsinized (Try) forms of L protein. *C*, Silver staining and immunoblot analysis of WT- and Try-BNC. After trypsin digestion, BNCs were purified by gel-filtration chromatography. The removal of N-terminal 125 aa was confirmed by immunoblotting with anti-S, anti-pre-S1, and anti-pre-S2 antibodies. Arrow and arrowhead indicate WT- and Try-L proteins, respectively. *D*, Typical fusion kinetics of Try-BNC. *, $p < 0.05$ by student's *t*-test.

2.3.2. pH-dependency of the fusogenic activity of BNCs

In duck HBV, the fusogenic domain is hidden within the L protein, but is exposed via spontaneous conformational change at a low pH [19]. This change is considered to contribute to the endosomal escape of duck HBV. I therefore performed the lipid-mixing assay of BNCs under low-pH conditions (from pH 7.5 to pH 4.5). As shown in Fig. 2.2A, membrane fusion induced by BNCs was enhanced by the decreasing pH, indicating that the fusogenic activity of BNCs is indeed dependent on low pH. To investigate whether the conformational change in the HBsAg L protein enhanced the fusogenic activity of BNCs at low pH, I performed the lipid-mixing assay using fixed BNCs, in which the pre-S regions were immobilized with 4% paraformaldehyde and 1% glutaraldehyde. The low pH-dependency of the BNC fusogenic activity was reduced by this fixation (Fig. 2.2B).

Next, to examine whether the N-terminal half of the pre-S1 region is involved in the low pH-dependent fusogenic activity, I evaluated the capacity of BNCs for binding to anti-pre-S1 antibodies by QCM. As shown in Fig. 2.2C, the amount of bound anti-pre-S1 antibodies was significantly increased at low pH (pH 5.5), suggesting that the pre-S1 regions of BNC are deployed to the outside of BNC under low pH conditions (Fig. 2.2D). Taken together, it appears that the low pH-dependent conformational change of the pre-S1 region contributes to the enhancement of fusogenic activity, presumably resulting in the endosomal escape of BNCs, as well as HBV, in late endosomes [4,5].

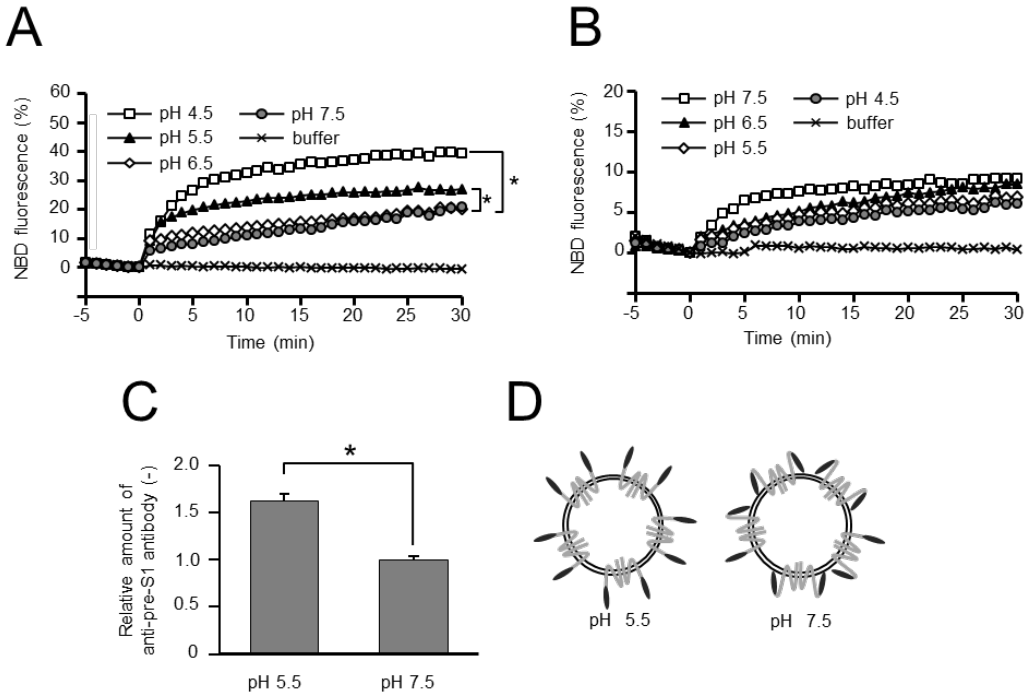

Fig. 2.2 Low pH-dependent fusogenic activity of BNCs. *A & B,* Typical fusion kinetics of non-treated (*A*) and fixed (*B*) BNCs under acidic conditions. *C,* Quartz crystal microbalance (QCM) measurements of anti-pre-S1 antibody-binding to BNCs under different pH conditions. Data obtained at pH 7.5 were defined as 1. *Bars,* S.D. (N = 3). *D,* Hypothetical model of low pH-dependent conformational change of L protein. *, $p < 0.05$ by the Student's *t*-test.

2.3.3. Delineation of the fusogenic domain in the pre-S1 region

Three peptides (24 aa) derived from the N-terminal 50 aa of the pre-S1 region (Fig. 2.3A) were chemically synthesized in a C-terminally His6-tag-fused form, and displayed on the surface of non-probe LPs through Ni-chelating phospholipids (DOGS-NTA-Ni). The lipid-mixing assay commenced with the addition of each synthetic peptide to the mixture of probe LPs and Ni-bearing non-probe LPs. As shown in Fig. 2.3B, peptide #1, encompassing aa 1–24 of pre-S1, showed strong fusogenic activity. The extent of membrane fusion at 30 min was about 25% of that induced by HIV-TAT peptide (positive control). The extent of membrane fusion at 30 min increased with the amounts of peptide #1 (1.0–20 μM), in a dose-dependent manner (Fig. 2.3C).

Since the synthetic peptide encompassing aa 2–39 of the pre-S1 region was shown to inhibit the hepatocellular infection by HBV [20], I next examined whether BNC-mediated membrane fusion is suppressed by an excess amount of peptide #1. As shown in Fig. 2.3D, the extent of membrane fusion induced by BNCs was significantly decreased by peptide #1 in a

dose-dependent manner, whereas no significant change was observed with an equal amount of peptide #2. Moreover, a shorter form of peptide #1, encompassing aa 9–24 of the pre-S1 region (#1ΔN8), showed comparable levels of fusogenic activity to peptide #1 (Fig. 2.3E). When two mutations were introduced into the well-conserved Phe residues of peptide #1ΔN8 (Phe-13 and Phe-14 changed to Gly-13 and Gly-14, #1ΔN8(F13/14A)), the mutated peptide did not show substantial levels of fusogenic activity. Taken together, these results show the N-terminal 16 aa of the pre-S1 region (NPLGFFPDHQLDPAFG) are crucial for BNC-mediated fusogenic activity.

Many viruses are taken up by target cells via receptor-dependent endocytosis. Some of them (*e.g.*, influenza virus, alphavirus, and flavivirus) undergo spontaneous conformational changes of their fusogenic peptides at low pH in the late endosomes, which triggers the fusion between the endosomal membrane and the viral envelope membrane [21–24]. In HBV, two fusogenic domains have been identified in the N-terminal part of the HBsAg S protein [25–27] and the C-terminal part of the HBsAg pre-S2 region [28] . These sequences are highly conserved among different HBV subtypes, and to a lesser extent among other members of the hepadonavirus family. The former fusogenic domain was also activated at low pH [29] . The pre-S1 region of the HBsAg L protein enhances membrane fusion under acidic conditions in the late endosomes, as do other domains in the pre-S2 region and S protein, and induces the rapid endosomal escape of HBV. However, as shown in Fig. 1D, the fusogenic domain of the pre-S1 region may be indispensable for HBV-induced membrane fusion. When HB patient-derived HBsAg (a mixture of the endogenous S, M, and L proteins) was used for the lipid-mixing assay, the fusogenic activity was found to be comparable to that obtained with BNCs (data not shown), implying that BNC shares the membrane fusion machinery with HBV. Furthermore, the activity substantially diminished when antibodies against the N-terminal part of the pre-S1 region were added (data not shown), corroborating that the pre-S1 region plays a central role in the membrane fusion of BNC and HBV.

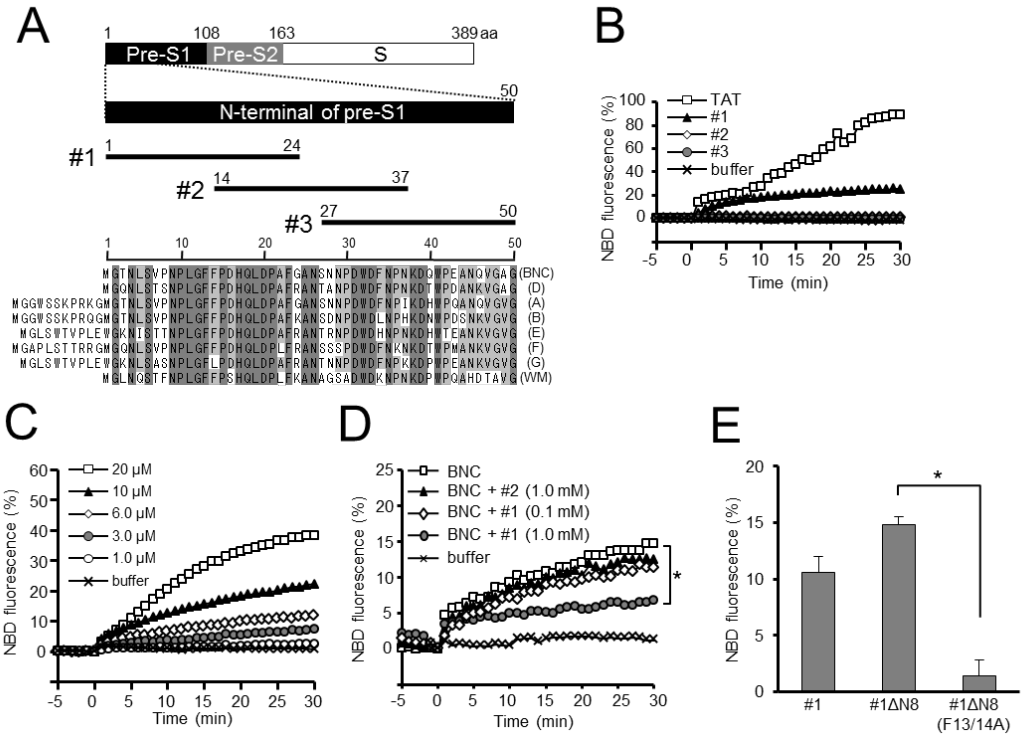

Fig. 2.3 Fusogenic activities of the amino-terminal sequence of the pre-S1 region. *A* (*upper*), pre-S1 region-derived synthetic peptides. Three peptides (#1–#3) were synthesized as a C-terminally His6 tag-fusion. *A* (*lower*), Alignment of different HBV pre-S1 sequences [30]: letters in parentheses indicate HBV genotype. WM indicates woolly monkey HBV. Identical amino acids are highlighted by boxes in dark gray; conserved amino acids are highlighted in light gray. *B,* Fusion kinetics of labeled LPs and DOGS-NTA-Ni-containing non-labeled LPs upon the addition of synthetic peptides. *C,* Fusion kinetics of these LPs upon the addition of 1–20 μM peptide #1. *D,* Fusion kinetics of these LPs upon the addition of BNCs in the presence of excess amounts of peptides #1 and #2. *E,* Fusion efficiency (at 5 min) of peptide #1, peptide #1 lacking the N-terminal 8 amino acids (peptide #1ΔN8), and peptide #1ΔN8 harboring two mutated amino acids (peptide #1ΔN8(F13/14A)). *Bars,* S.D. (N = 3). *, $p < 0.05$ by the Student's *t*-test.

2.3.4. Cellular uptake of BNC–LP-bead complexes

The identification of the low pH-dependent fusogenic activity of the pre-S1 region of L protein led us to prepare BNC–LP–beads complexes by mixing BNCs with LPs containing 20-nm fluorescence beads (LP–beads) under acidic conditions (pH 4.0). As shown in Table 2.1, BNC–LP complexes showed 150-200 nm diameter and negative surface charges (-35 ~ -50 mV). For accessing hepatocytes in vivo, the BNC–LP complexes should pass through the sinusoidal

endothelial fenestrae. Since the pore size of fenestrae in human is ranging from 60 to 200 nm [31], it is considered that the systemically administrated BNC–LP complexes could pass through the fenestrae and reach at hepatocytes in human liver.

Table 2.1 Properties of complexes

Samples	Z-average (d.nm)	PdI	ζ-potential (mV)
20 nm-beads	30.1 ± 3.23	0.090	-31.2 ± 10.7
LP	77.8 ± 2.94	0.081	-70.7 ± 6.11
LP-beads	111 ± 0.53	0.310	-57.8 ± 9.79
BNC-LP-beads	154 ± 4.93	0.278	-44.0 ± 7.10
BNC-LP-Au NPs	182 ± 21.1	0.138	-34.8 ± 1.20

N=3, ±SD

When BNC–LP–bead complexes were incubated with various cells for 60 min, they bound more efficiently than LP–beads to human hepatic cell-derived cell lines (Huh7 and HepG2 cells), but not to other cell lines (Fig. 2.4A); the cell-specificity of the bead complex was very similar to those of BNCs and BNC–LP complexes [4,5,8]. Over a period of 24 h, the amount of BNC–LP–bead complex bound and internalized to Huh7 cells increased with time (Fig. 2.4B and C). After 24-h incubation, the amount of bound complex was 15-times higher than that of LP–beads.

After liberating cell surface-bound complexes by trypsinization, the amount of internalized BNC–LP–beads complexes increased proportionally during the 24 h incubation (Fig. 2.4D). These results indicated that BNCs endow LPs not only with human hepatic cell-specificity, by means of the human hepatocyte-recognition domain of the pre-S1 region, but also with cell-entering activity, presumably due to the fusogenic domains.

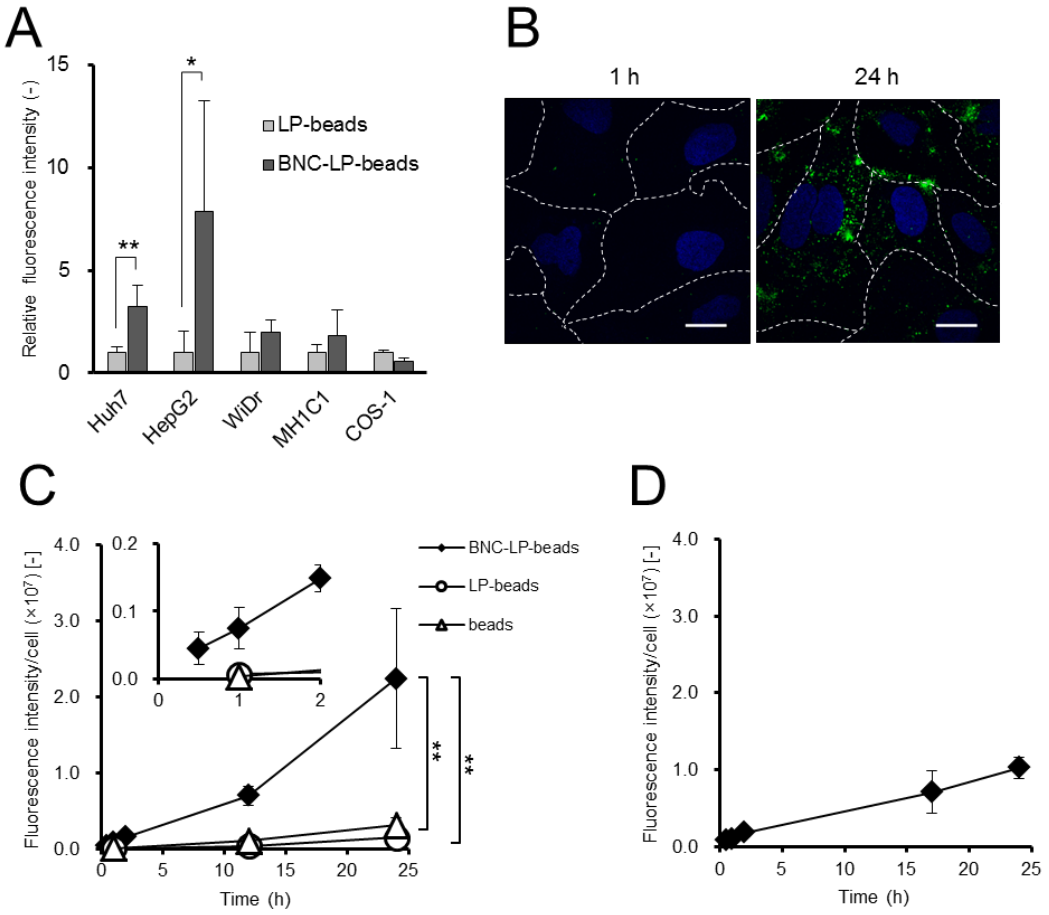

Fig. 2.4 Binding and internalization of BNC–LP–bead complexes. BNC–LP–bead complexes were incubated with various cell types, followed by fixation and fluorescent imaging. *A*, The amount of BNC–LP–bead complexes bound to cells after 60-min incubation. Fluorescence intensities per cell were quantified and normalized to the value of LP–beads (set as 1.0). *B*, The binding and uptake of BNC–LP–bead complexes to Huh7 cells. BNC–LP–bead complexes were incubated with Huh7 cells for 1 and 24 h. Green and blue dots represent beads and nuclei, respectively. Dashed lines represent the plasma membrane. Bars, 20 μm. *C*, The binding and uptake kinetics of BNC–LP–bead complexes in *B*. *D*, Internalization kinetics of BNC–LP–bead complexes in Huh7 cells. Values, mean ± S.D. (N = 5), *, $p < 0.05$, **, $p < 0.01$ by the Student's *t*-test against BNC–LP–beads.

2.3.5. Intracellular trafficking of BNC–LP complexes

Huh7 cells treated with BNC–LP–bead complexes for particular periods of time (1, 6, and 24 h) were stained with Lysotracker Red, which can stain the acidic sub-cellular compartments (*i.e.*, late endosomes and lysosomes), after which the cell surface-bound complexes were liberated by trypsinization. As shown in Fig. 2.5A and B, most of the beads did not colocalize with Lysotracker

Red during 24 h. Under the same conditions, epidermal growth factor (EGF) was internalized and mostly localized in lysosomes [32], suggesting that BNC–LP–bead complexes are internalized by endocytosis and then deliver their payloads to the cytoplasm.

To investigate the pathway by which BNC–LP complexes are taken up, the cells were treated with the endocytosis inhibitors chlorpromazine [33], and amiloride [34], to inhibit clathrin-mediated endocytosis and macropinocytosis, respectively. Most human hepatocellular carcinoma-derived cell lines are known to lack caveolin [35]. The treatment with chlorpromazine significantly reduced the amounts of beads, LPs, and BNCs in the intracellular fraction, while amiloride treatment had no effect (Fig. 2.5C), indicating that BNC–LP–bead complexes were taken up mainly via clathrin-mediated endocytosis, but not by macropinocytosis. In contrast, the uptake of intact LPs was significantly reduced by the treatment with amiloride, but not with chlorpromazine, indicating that LPs were taken up by non-selective endocytosis, *i.e.*, macropinocytosis [36]. Thus, I postulated that the surface modification of BNCs could alter the uptake pathway of LPs from macropinocytosis (non-selective, inefficient) to clathrin-mediated endocytosis (receptor-mediated, efficient) by means of the human hepatocyte-recognition domain of the pre-S1 region.

To date, it has been believed that HBV enters target cells by receptor-mediated endocytosis, moves to the late endosomes, fuses with the endosomal membrane, and then translocates to the cytoplasm with the concurrent release of nucleocapsid particles [25,37]. The low pH-dependent fusogenic activity of the 9–24 aa of the pre-S1 region (*see* section 2.3.3) may contribute to the endosomal escape of nucleocapsid particles. Similar machinery would be operative in the cytoplasmic delivery of payloads from the BNC–LP complexes in late endosomes.

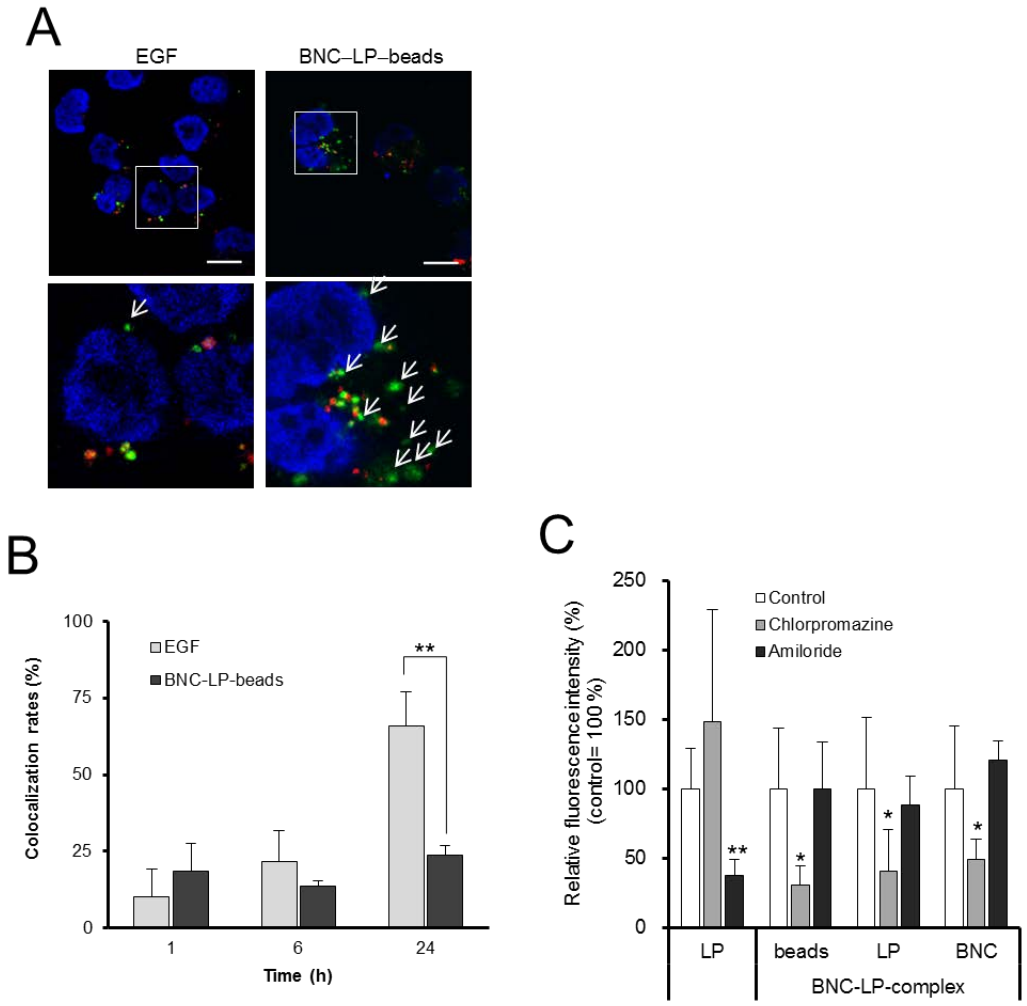

Fig. 2.5 Intracellular localization and uptake pathway of BNC–LP–bead complexes. *A*, Fluorescence images of EGF- or BNC–LP–bead complex-treated Huh7 cells (24 h incubation). Green, red, and blue dots represent EGF or beads, Lysotracker Red, and nuclei, respectively. Lower panels show magnified images of upper panels. Arrows indicate green dots that are not colocalized with red dots. Bars, 10 μm. *B*, Colocalization rates of EGF- or BNC–LP–bead complexes with Lysotracker Red. *C*, Effect of endocytosis inhibitors. Huh7 cells were pretreated with chlorpromazine (12.5 μg/ml, 30 min) or amiloride (1 mM, 15 min), and then incubated with BNC–LP–bead complexes (labeled with CF488 for BNCs, rhodamine for LPs) or rhodamine-labeled LPs for 30 min. All values were normalized to control values (set as 100%). Values are mean ± S.D. ($N \geq 4$), *, $p < 0.05$, **, $p < 0.01$ by the Student's *t*-test against the control.

By the lipid mixing assay (*see* Fig. 2.1), BNC–LP complexes were also shown to have low pH-dependent fusogenic activity (Fig. 2.6A). Therefore, I exploited whether the fusogenic activity of BNC or BNC-LP complexes cause membrane disruption of LPs containing pyranine and DPX

(fluorescence quencher) under low-pH conditions. As shown in Fig. 2.6B, both materials could disrupt exogenous LPs in a low-pH dependent manner, probably owing to the membrane fusogenic region of L protein. Next, the payloads release of BNC-LP complexes was examined by using doxorubicin (DOX) as a model payload. After remote loading of DOX into the complexes, the BNC-LP-DOX complexes and LP-DOX complexes (control) were contacted with free LPs under low-pH conditions. The DOX release was observed only in BNC-LP-DOX complexes, which was enhanced by low pH and free exogenous LPs synergistically (Fig. 2.6C). These results indicated that BNC-LP complexes could induce membrane disruption of exogenous LPs and themselves in low pH-dependent manner. Taken together, it was postulated that the BNC-LP complexes in late endosomes could release payloads into cytoplasm through the disruption of endosomal membrane.

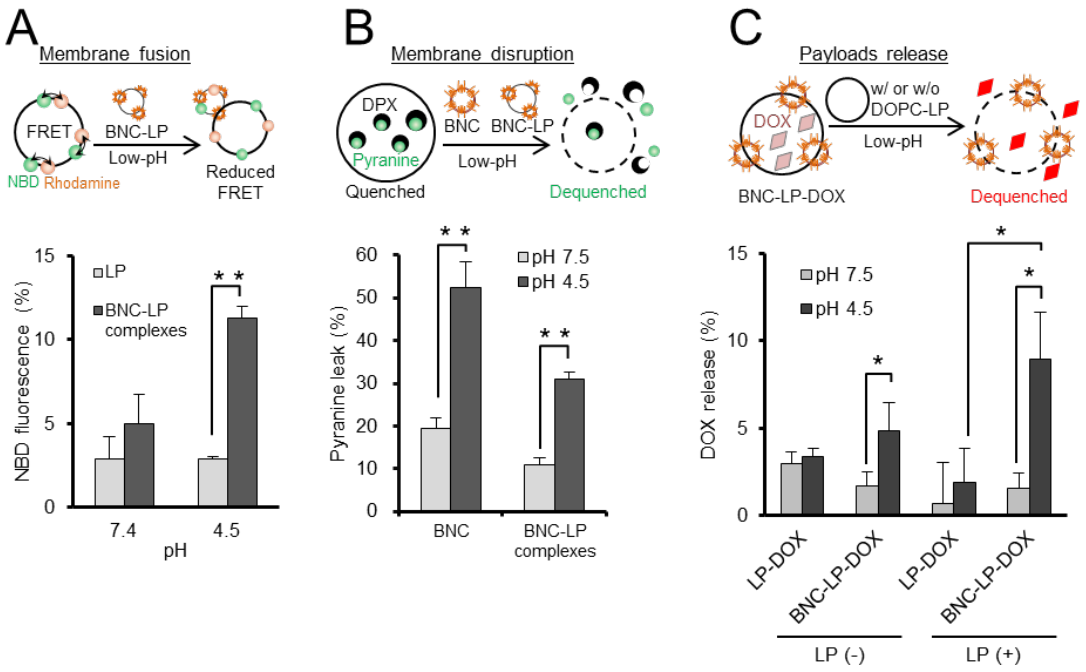

Fig. 2.6 Membrane fusion, membrane disruption, and payloads release of BNC–LP complexes under low-pH conditions. *A*, Fusogenic activity of BNC-LP complexes. Probe LPs (10 μg) containing NBD and rhodamine were incubated with no-probe LPs (40 μg) and BNC–LP complexes (40 μg as lipids) at pH 7.4 and pH 4.5 at 37ºC for 30 min. *B*, Membrane disruption activity of BNC–LP complexes. LPs (4 μg) containing pyranine and DPX were incubated with BNC (1 μg as protein) and BNC–LP complexes (1 μg as protein) at pH 7.4 and pH 4.5 at 37ºC for 30 min. *C*, Payload release from BNC–LP–DOX complexes (10 μg as LPs). The complexes were incubated with or without LPs (20 μg) at pH 7.4 and pH 4.5 at 37ºC for 30 min. *Bars*, S.D. (N = 3). *, $p < 0.05$, **, $p < 0.01$ by the Student's *t*-test.

2.3.6. Intracellular localization of BNC–LP–Au nanoparticles complexes

In order to decipher the intracellular localization of payloads of BNC–LP complexes, ~8-nm Au nanoparticles (NPs) were encapsulated in BNC–LP complexes in a manner similar to that used with beads. Huh7 cells were incubated with the complexes for 26 h, which allowed us to identify the final intracellular destination of Au NPs. The cells were fixed, negatively stained with uranyl acetate, and observed by TEM. As shown in Fig. 2.7, Au NPs were detected as dense dots. Some Au NPs were found to localize in the cytoplasm, because no membrane structure was apparent around them (Fig. 2.7B, and C). Other Au NPs localized mainly to the late endosomes (Fig. 2.7D and E). These results corroborated that BNC–LP complexes were internalized into cells by means of clathrin-mediated endocytosis; some parts fused with the membrane of the late endosomes, and, finally, the payloads were released from the endocytic vesicles to the cytoplasm.

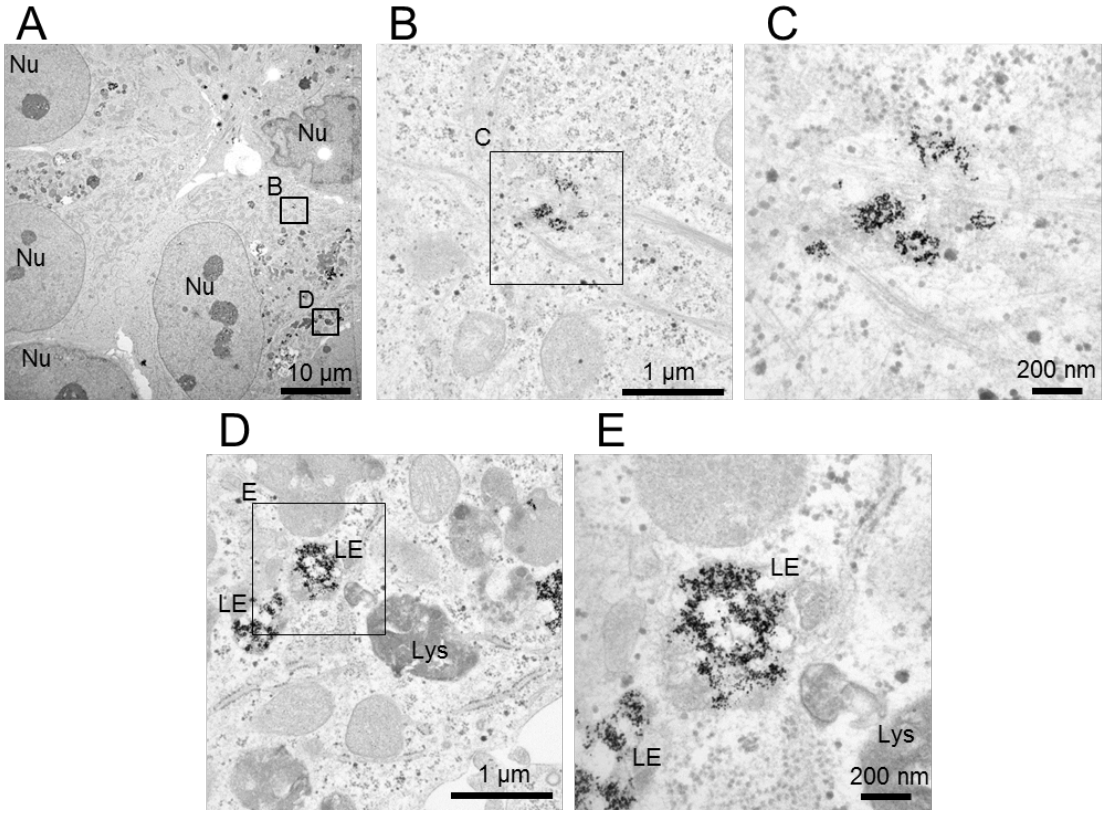

Fig. 2.7 Transmission electron microscopic observation of BNC–LP–Au nanoparticle (NP) complexes in Huh7 cells. Nu, nucleus; LE, late endosomes; and Lys, lysosomes.

2.4. Conclusion

Two types of HBV receptors have been proposed to be involved in the early infection mechanism, such as heparin sulfate proteoglycan, as a low-affinity receptor [38], and an unidentified molecule, as a high-affinity receptor, which has recently been proposed to be the sodium

taurocholate-cotransporting polypeptide [39]. The former receptor initially interacts with HBV, and promptly transfers HBV to the latter receptor, followed by virus internalization by receptor-mediated endocytosis. In this study, novel low pH-dependent fusogenic activity was identified in the pre-S1 region (9–24 aa) of HBV/BNC, using a lipid-mixing assay; this region was postulated to play a central role in the uncoating of HBV in endosomes and the subsequent cytoplasmic delivery of nucleocapsid particles. Similar to what has been demonstrated for BNCs [4], BNC–LP complexes may interact with both HBV receptors sequentially, become internalized by clathrin-mediated endocytosis, and release their payloads from the endosomes to the cytoplasm by the action of the fusogenic domain (Fig. 2.8). Since many viruses can establish an infection of host cells by means of their envelope proteins [40], LPs displaying such proteins hold promise as nanocarriers for the cytoplasmic delivery of drugs and genes with high specificity and infectivity.

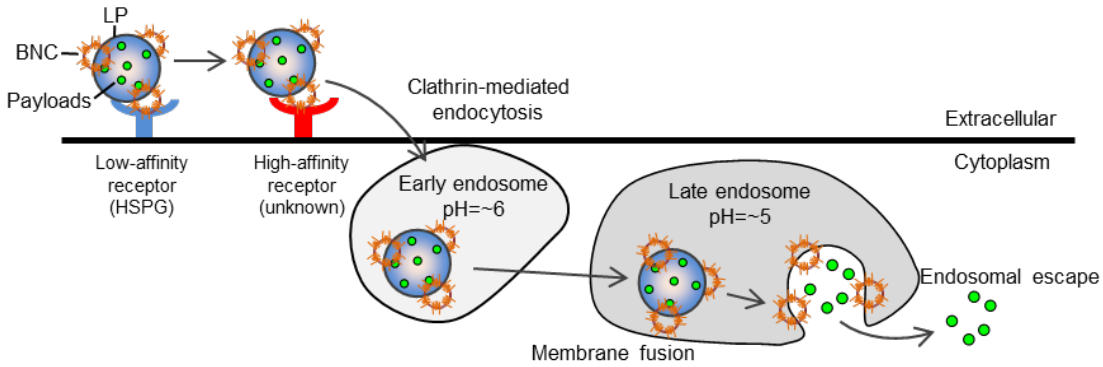

Fig. 2.8 Cell entry, intracellular trafficking, and subsequent payload release of BNC–LP complexes. First, BNC–LP complexes bind to heparin sulfate proteoglycan (HSPG) and are promptly transferred to the high-affinity receptor, after which they enter into the cells via clathrin-mediated endocytosis. After enhancement of the pH-dependent fusogenic activity of the pre-S1 region in late endosomes (~pH 5), BNC–LP complexes fuse with and disrupt endosomal membranes, and then subsequently release their payloads into the cytoplasm.

2.5. References

[1] A.R. Neurath, S.B. Kent, N. Strick, K. Parker, Identification and chemical synthesis of a host cell receptor binding site on hepatitis B virus., Cell. 46 (1986) 429–436. doi:0092-8674(86)90663-X [pii].

[2] S. Kuroda, S. Otaka, T. Miyazaki, M. Nakao, Y. Fujisawa, Hepatitis B virus envelope L protein particles: Synthesis and assembly in Saccharomyces cerevisiae, purification and

characterization, J. Biol. Chem. 267 (1992) 1953–1961. http://www.ncbi.nlm.nih.gov/pubmed/18434744.

[3] T. Yamada, H. Iwabuki, T. Kanno, H. Tanaka, T. Kawai, H. Fukuda, et al., Physicochemical and immunological characterization of hepatitis B virus envelope particles exclusively consisting of the entire L (pre-S1 + pre-S2 + S) protein, Vaccine. 19 (2001) 3154–3163. doi:10.1016/S0264-410X(01)00017-2.

[4] M. Yamada, A. Oeda, J. Jung, M. Iijima, N. Yoshimoto, T. Niimi, et al., Hepatitis B virus envelope L protein-derived bio-nanocapsules: mechanisms of cellular attachment and entry into human hepatic cells., J. Control. Release. 160 (2012) 322–9. doi:10.1016/j.jconrel.2011.11.004.

[5] T. Yamada, Y. Iwasaki, H. Tada, H. Iwabuki, M.K.L. Chuah, T. VandenDriessche, et al., Nanoparticles for the delivery of genes and drugs to human hepatocytes., Nat. Biotechnol. 21 (2003) 885–90. doi:10.1038/nbt843.

[6] Y. Iwasaki, M. Ueda, T. Yamada, a Kondo, M. Seno, K. Tanizawa, et al., Gene therapy of liver tumors with human liver-specific nanoparticles., Cancer Gene Ther. 14 (2007) 74–81. doi:10.1038/sj.cgt.7700990.

[7] Y. Kaneda, Virosomes: Evolution of the liposome as a targeted drug delivery system, Adv. Drug Deliv. Rev. 43 (2000) 197–205. doi:10.1016/S0169-409X(00)00069-7.

[8] J. Jung, T. Matsuzaki, K. Tatematsu, T. Okajima, K. Tanizawa, S. Kuroda, Bio-nanocapsule conjugated with liposomes for in vivo pinpoint delivery of various materials., J. Control. Release. 126 (2008) 255–64. doi:10.1016/j.jconrel.2007.12.002.

[9] J. Jung, M. Iijima, N. Yoshimoto, M. Sasaki, T. Niimi, K. Tatematsu, et al., Efficient and rapid purification of drug- and gene-carrying bio-nanocapsules, hepatitis B virus surface antigen L particles, from Saccharomyces cerevisiae., Protein Expr. Purif. 78 (2011) 149–55. doi:10.1016/j.pep.2011.04.008.

[10] G. Sauerbrey, The use of quartz oscillators for weighing thin layers and for microweighing, Z. Phys. 155 (1959) 206–222. doi:10.1007/BF01337937.

[11] H.T.S. Britton, R.A. Robinson, CXCVIII. Universal Buger Solutions and the Dissociation Constant of Veronal, J. Chem. Soc. (1923) 1456–1462. doi:10.1039/JR9310001456.

[12] T. Kasuya, J. Jung, R. Kinoshita, Y. Goh, T. Matsuzaki, M. Iijima, et al., Bio-Nanocapsule-Liposome Conjugates for In Vivo Pinpoint Drug and Gene Delivery, Methods Enzymol. 464 (2009) 147–166. doi:10.1016/S0076-6879(09)64008-8.

[13] X. Li, D.J. Hirsh, D. Cabral-Lilly, A. Zirkel, S.M. Gruner, A.S. Janoff, et al., Doxorubicin physical state in solution and inside liposomes loaded via a pH gradient, Biochim. Biophys. Acta - Biomembr. 1415 (1998) 23–40. doi:10.1016/S0005-2736(98)00175-8.

[14] E. Yuba, A. Harada, Y. Sakanishi, S. Watarai, K. Kono, A liposome-based antigen delivery system using pH-sensitive fusogenic polymers for cancer immunotherapy., Biomaterials. 34 (2013) 3042–52. doi:10.1016/j.biomaterials.2012.12.031.

[15] H. Ellens, J. Bentz, F.C. Szoka, H+- and Ca2+-induced fusion and destabilization of liposomes., Biochemistry. 24 (1985) 3099–3106. doi:10.1021/bi00334a005.

[16] J. Bhattacharya, U. Choudhuri, O. Siwach, P. Sen, A.K. Dasgupta, Interaction of hemoglobin and copper nanoparticles: implications in hemoglobinopathy., Nanomedicine. 2 (2006) 191–9. doi:10.1016/j.nano.2006.07.001.

[17] V.S. Malinin, P. Frederik, B.R. Lentz, Osmotic and curvature stress affect PEG-induced fusion of lipid vesicles but not mixing of their lipids., Biophys. J. 82 (2002) 2090–100. doi:10.1016/S0006-3495(02)75556-2.

[18] S.M. Dennison, M.E. Bowen, A.T. Brunger, B.R. Lentz, Neuronal SNAREs do not trigger fusion between synthetic membranes but do promote PEG-mediated membrane fusion., Biophys. J. 90 (2006) 1661–75. doi:10.1529/biophysj.105.069617.

[19] E.V.L. Grgacic, H. Schaller, A Metastable Form of the Large Envelope Protein of Duck Hepatitis B Virus: Low-pH Release Results in a Transition to a Hydrophobic, Potentially Fusogenic Conformation, J. Virol. 74 (2000) 5116–5122. doi:10.1128/JVI.74.11.5116-5122.2000.

[20] J. Petersen, M. Dandri, W. Mier, M. Lütgehetmann, T. Volz, F. von Weizsäcker, et al., Prevention of hepatitis B virus infection in vivo by entry inhibitors derived from the large envelope protein., Nat. Biotechnol. 26 (2008) 335–341. doi:10.1038/nbt1389.

[21] J. White, Membrane fusion, Science (80-.). 258 (1992) 917–924. doi:10.1126/science.1439803.

[22] F.M. Hughson, Structural characterization of viral fusion proteins, Curr. Biol. 5 (1995) 265–274. doi:10.1016/S0960-9822(95)00057-1.

[23] M. Kielian, F. a Rey, Virus membrane-fusion proteins: more than one way to make a hairpin., Nat. Rev. Microbiol. 4 (2006) 67–76. doi:10.1038/nrmicro1326.

[24] S.C. Harrison, Viral membrane fusion., Nat. Struct. Mol. Biol. 15 (2008) 690–8. doi:10.1038/nsmb.1456.

[25] X. Lu, T. Block, Study of the early steps of the Hepatitis B Virus life cycle, Int. J. Med. Sci. 1 (2004) 21–33.

[26] Cooper, A, The earliest steps in hepatitis B virus infection, Biochim. Biophys. Acta - Biomembr. 1614 (2003) 89–96. doi:10.1016/S0005-2736(03)00166-4.

[27] I. Rodriguez-Crespo, J. Gomez-Gutierrez, M. Nieto, D.L. Peterson, F. Gavilanes, Prediction of a putative fusion peptide in the S protein of hepatitis B virus, J. Gen. Virol. 75 (1994) 637–639. doi:10.1099/0022-1317-75-3-637.

[28] S. Oess, E. Hildt, Novel cell permeable motif derived from the PreS2-domain of hepatitis-B virus surface antigens., Gene Ther. 7 (2000) 750–758. doi:10.1038/sj.gt.3301154.

[29] I. Rodriguez-Crespo, E. Nunez, J. Gomez-Gutierrez, B. Yelamos, J.P. Albar, D.L. Peterson, et al., Phospholipid interactions of the putative fusion peptide of hepatitis B virus surface antigen S protein, J. Gen. Virol. 76 (1995) 301–308. doi:10.1099/0022-1317-76-2-301.

[30] M. Engelke, K. Mills, S. Seitz, P. Simon, P. Gripon, M. Schnölzer, et al., Characterization of a hepatitis B and hepatitis delta virus receptor binding site., Hepatology. 43 (2006) 750–60. doi:10.1002/hep.21112.

[31] E. Wisse, F. Jacobs, B. Topal, P. Frederik, B. De Geest, The size of endothelial fenestrae in human liver sinusoids: implications for hepatocyte-directed gene transfer., Gene Ther. 15 (2008) 1193–9. doi:10.1038/gt.2008.60.

[32] C.E. Futter, A. Pearse, L.J. Hewlett, C.R. Hopkins, Multivesicular endosomes containing internalized EGF-EGF receptor complexes mature and then fuse directly with lysosomes, J. Cell Biol. 132 (1996) 1011–1023. doi:10.1083/jcb.132.6.1011.

[33] L.H. Wang, K.G. Rothberg, R.G.W. Anderson, Mis-assembly of clathrin lattices on endosomes reveals a regulatory switch for coated pit formation, J. Cell Biol. 123 (1993) 1107–1117. doi:10.1083/jcb.123.5.1107.

[34] M.A. West, S. Bretscher, Distinct endocytotic pathways in epidermal growth factor-stimulated human carcinoma A431 cells [published erratum appears in J Cell Biol 1990 Mar;110(3):859], J. Cell Biol. 109 (1989) 2731–2739. doi:10.1083/jcb.109.6.2731.

[35] R. Mayoral, A.M. Valverde, C. Llorente Izquierdo, A. González-Rodríguez, L. Boscá, P. Martín-Sanz, Impairment of transforming growth factor beta signaling in caveolin-1-deficient hepatocytes: role in liver regeneration., J. Biol. Chem. 285 (2010) 3633–42. doi:10.1074/jbc.M109.072900.

[36] J.A. Swanson, C. Watts, Macropinocytosis., Trends Cell Biol. 5 (1995) 424–428. doi:10.1016/S0962-8924(00)89101-1.

[37] S. Schädler, E. Hildt, HBV life cycle: Entry and morphogenesis, Viruses. 1 (2009) 185–209. doi:10.3390/v1020185.

[38] A. Schulze, P. Gripon, S. Urban, Hepatitis B virus infection initiates with a large surface protein-dependent binding to heparan sulfate proteoglycans., Hepatology. 46 (2007) 1759–68. doi:10.1002/hep.21896.

[39] H. Yan, G. Zhong, G. Xu, W. He, Z. Jing, Z. Gao, et al., Sodium taurocholate cotransporting polypeptide is a functional receptor for human hepatitis B and D virus., Elife. 1 (2012) e00049. doi:10.7554/eLife.00049.

[40] J. Schneider-Schaulies, Cellular receptors for viruses: links to tropism and pathogenesis., J. Gen. Virol. 81 (2000) 1413–29. http://www.ncbi.nlm.nih.gov/pubmed/10811925.

Chapter III One-step scalable preparation method for non-cationic liposomes with high siRNA content

3.1. Introduction

Nucleic acid therapeutics are promising and potent therapeutics, because they could modulate the expression of genes responsible for disease onset. While most conventional low-molecular weight medicines execute their functions at the cell surface, nucleic acid therapeutics could directly modulate the intracellular events that cause disease. In particular, many clinical trials have sought to use short interfering RNAs (siRNAs), because they can suppress targeted genes at low doses [1]. However, siRNAs are easily degraded in the body via RNases in the blood, skin, and other organs. Furthermore, it is essential to deliver siRNAs to the site of disease in the body to obtain sufficient therapeutic efficacy.

To address these issues, siRNA encapsulation in nanocarriers has been utilized to protect siRNA from degradation and deliver siRNA to the cells and tissues of interest. For example, 100 nm nanocarriers accumulated spontaneously in tumors due to the enhanced permeability and retention effect [2], and evaded glomerular filtration, thereby maintaining their blood levels [3]. Cationic liposome (LPs), cationic polymer nanomicelles, and poly(lactic-co-glycolic acid) (PLGA) nanoparticles have been used for siRNA delivery *in vitro* and *in vivo* [4,5]. Due to the cationic charges on the LP and polymer surface, they could interact with anionic phosphate groups in siRNAs to spontaneously form stable complexes (referred to as lipoplexes and polyplexes, respectively) and transfect cells *in vitro* and *in vivo* [6,7]. However, the cationic charges can induce cytotoxicity [8], and the nanocarriers can be inactivated by nonspecific binding to cells or proteins [9]. Furthermore, perturbation of gene expression by cationic lipids is a considerable problem [10].

Non-cationic LPs are considered a safe nanocarrier for systemic siRNA delivery [11,12]. Several lines of research have demonstrated the possibility for efficient nucleic acid encapsulation in pre-formed non-cationic LPs. Semple *et al.* [13] reported that antisense DNA could be encapsulated in pH-sensitive LPs using ionizable lipid 1,2-dioleoyl-3-dimethylammonium-propane (DODAP), which was then modified to establish a lipid nanoparticle (LNP) technology for efficient systemic siRNA delivery [14] and used in human clinical trials [15]. Kapoor and Burgess [11,16] found that $CaCl_2$ could enhance siRNA encapsulation in pre-formed anionic LPs. Additionally, Landen *et al*. [17] reported that neutral LPs lyophilized in the presence of butanol and Tween 20 could encapsulate siRNA upon hydration. Finally, Bailey and Sullivan [18] reported that both ethanol and $CaCl_2$ could enhance the encapsulation of plasmid DNA into pre-formed neutral LPs. Although these methods could produce siRNA-containing LPs using either pre-formed neutral or pre-formed anionic LPs, they did not fulfill the criteria for manufacturing non-cationic LPs containing siRNA. First, LPs should be less than 200 nm for efficient systemic delivery. The siRNA content should also be high (>

10 wt% of LPs). Additionally, toxic solvents and materials should be avoided in the preparation. Finally, the method should be suitable for large-scale production, preferentially using a one-step protocol. These situations have led us to establish a new one-step method to prepare non-cationic LPs containing high siRNA levels.

3.2. Materials and Methods

3.2.1. Materials

1,2-Dioleoyl-*sn*-glycero-3-phosphocholine (DOPC), 1,2-dioleoyl-*sn*-glycero-3-phosphoethanolamine (DOPE), 1-palmitoyl-2-oleoyl-*sn*-glycero-3-phosphocholine (POPC), 1,2-dipalmitoyl-*sn*-glycero-3-phosphocholine (DPPC), 1,2-distearoyl-*sn*-glycero-3-phosphocholine (DSPC), 1,2-dipalmitoyl-*sn*-glycero-3-phosphoethanolamine (DPPE), 1,2-dipalmitoyl-*sn*-glycero-3-phosphoglycerol sodium salt (DPPG-Na), and N-(Carbonyl-methoxypolyethyleneglycol 2000)-1,2-dioleoyl-*sn*-glycero-3-phosphoethanolamine, sodium salt (DOPE-PEG2000) were purchased from NOF (Tokyo, Japan). Cholesterol was purchased from Sigma–Aldrich (St. Louis, MO, USA). 1,2-di-(9Z-hexadecenoyl)-*sn*-glycero-3-phosphocholine (16:1 [Δ9-cis] PC) and 1,2-di-(9E-octadecenoyl)-*sn*-glycero-3-phosphocholine (18:1 [Δ9-trans] PC) were purchased from Avanti Polar Lipids (Alabaster, AL, USA). GL3Luc siRNA (sense strand, 5′-CUUACGCUGAGUACUUCGAtt-3′; antisense strand, 5′-UCGAAGUACUCAGCGUAAGtt-3′; where lower cases indicate DNA) [19] was purchased from Gene Design Inc. (Osaka, Japan). Cholesterol-conjugated GL3Luc siRNA was purchased from Hokkaido System Science Co. (Sapporo, Japan). The cholesterol group was conjugated at 3′ end of the sense strand [20].

3.2.2. Encapsulation of siRNA into pre-formed LPs (sequential method)

Lipids dissolved in chloroform/methanol (2:1, volume) were added to a round bottom flask, evaporated to form thin film, and hydrated with 10 mM Tris-HCl buffer (pH 8.0), followed by the sonication in bath-type sonicator. The LP size was trimmed by extrusion with a 50 or 100 nm polycarbonate membrane to form 100 nm LPs. The encapsulation of siRNAs into the LPs was performed by the modified method published by Bailey and Sullivan [18]. The LP mixture (500 μg) and siRNAs (50 μg) in 300 μl Tris-HCl buffer were instilled with 200 μl of ethanol containing 10 mM $CaCl_2$ (final $CaCl_2$ concentration, 4 mM) with continuous vortexing at room temperature, followed by the dialysis against phosphate buffered saline (PBS, pH 7.4) overnight at 4°C.

3.2.3. Formation of siRNA-encapsulated LPs (simultaneous method)

A mixture of 6.7 mM $CaCl_2$ and siRNA (50 μg) in 300 μl Tris-HCl buffer was instilled with 200 μl ethanol containing lipids (500 μg) with continuous vortexing at room temperature, followed by dialysis against PBS (pH 7.4) overnight at 4°C.

3.2.4. Characterization of siRNA-encapsulated LPs

Encapsulation efficiency (EE) was determined using Quant-iT RiboGreen RNA Reagent (Life Technologies, Carlsbad, CA, USA) according to the method reported by Heyes [21]. EE was calculated as follows: EE (%) = ($[C_{total}]$-$[C_{free}]$)/(C_{total}) × 100, where C_{free} is the siRNA concentration without Triton X-100 (TX-100) treatment, C_{total} is the siRNA concentration with 0.1% (v/v) TX-100 treatment. The LP concentrations were calibrated by the amounts of phospholipid and cholesterol, which were determined with the Wako Diagnostics-Phospholipids Reagent (Wako, Osaka, Japan) and Wako Diagnostics-Total Cholesterol Reagent (Wako), respectively. The LP size in PBS was measured at 25°C by dynamic light scattering analysis using a Zetasizer Nano ZS (Malvern, Worcestershire, UK). The LP ζ-potential in PBS was measured at 25°C by laser Doppler micro-electrophoresis using a Zetasizer Nano ZS.

3.2.5. Evaluation of stability of siRNA-encapsulated LP

To evaluate resistance against RNase digestion, LPs containing 100 ng siRNA were incubated in 50% (v/v) fetal bovine serum (FBS) as a source of RNase at 37°C for 30 min, disrupted with 0.1% TX-100, and then analyzed by 2% agarose gel electrophoresis. The gel was stained with ethidium bromide and visualized under ultraviolet illuminator FAS III (TOYOBO, Osaka, Japan).

3.2.6. Cytotoxicity of siRNA-encapsulated LPs

The human hepatocellular carcinoma line HepG2 (Riken Cell Bank, Tsukuba, Japan) was seeded in a 96-well plate (approx. 5.0×10^3 cells/well) and cultured in Dulbecco's modified Eagle's medium supplemented with 10% FBS in a humidified 5% (v/v) CO_2 atmosphere at 37°C. Cells were treated with the indicated concentrations of LPs containing siRNA for 24 h. Cell viability was measured with the WST-8 reagent (Nacalai Tesque, Kyoto, Japan).

3.2.7. Transfection of siRNA-encapsulated LPs conjugated with bio-nanocapsules (BNC-LP-siRNA)

Bio-nanocapsules (BNCs), hepatitis B virus (HBV) envelop L protein particles, were overexpressed in yeast cells [22], and then purified homogeneously as described previously[23]. To vest the targeting ability to the siRNA-encapsulated LPs (DPPC/DPPE/DPPG-Na/cholesterol, 15/15/30/40 [mol/mol/mol/mol]), the LP-siRNA complexes (containing GL3Luc siRNA, siRNA/LP = 2.17 wt%) were mixed with BNC at one-twentieth weight of LPs to form BNC-LP-siRNA complexes [24]. Briefly, the mixture of LPs and BNCs were incubated in Britton Robinson buffer

(pH = 4) [25] at 60°C for 90 min, and applied onto size-exclusion chromatography (Sephadex G-25, GE healthcare, Little Chalfont, UK). Human hepatocellular carcinoma cell line Huh7 (Riken Cell Bank) expressing firefly luciferase gene (approx. 2.5×10^4 cells/well in 24-well plate) was cultured with the BNC-LP-siRNA complexes (final siRNA concentration, 150 nM) for 24 h, followed by luciferase assay using Steady-Glo Luciferase Assay System (Promega, Madison, WI, USA). Luciferase expression level was normalized by the protein concentration of cell lysate using BCA Protein Assay kit (Life Technologies). DharmaFECT (GE healthcare) was used as a positive control for siRNA transfection (final siRNA concentration, 100 nM).

3.2.8. Intracellular localization of BNC-LP-siRNA complexes

As a model of siRNA, double-strand DNA (dsDNA) corresponding to GL3Luc siRNA was synthesized, followed by the conjugation with 6-carboxyfluorescein (6-FAM) at 5'-end of the sense strand and cholesterol at 3'-end of the sense strand (Gene Design Inc.). The dsDNA (hereafter, referred to as FAM-chol-dsDNA) was encapsulated into BNC-LP complexes as described above. Huh7 cells (approx. 1.0×10^4 cells/well in 8-well glass-bottomed chamber slide) were incubated with BNC-LP- FAM-chol-dsDNA complexes (final dsDNA concentration, 1.1 μM) at 37 °C for 24 h, followed by staining with 50 nM of LysoTracker Red (Life technologies) at 37 °C for 30 min, wash with PBS, fixation with 4% (w/v) paraformaldehyde at room temperature for 20 min, and staining with Hoechst 33342 at room temperature for 20 min. As a positive control, Lipofectamine RNAiMAX Transfection reagent (Life Technologies) was used. Cells were observed under a confocal laser scanning microscope (FV1000D; Olympus; Tokyo, Japan).

3.3. Results and discussion

3.3.1. siRNA encapsulation into pre-formed neutral LPs (sequential method)

As previously described, siRNA was encapsulated into pre-formed neutral LPs composed of 100 mol% DOPC or 50/50 mol% DOPC/DOPE in the presence of 40 vol% ethanol and 4 mM $CaCl_2$ (hereafter, referred to as sequential method) [18]. As shown in Table 3.1, up to 80 and 60 wt% of the siRNAs were encapsulated in the LPs composed of DOPC and DOPC/DOPE, respectively. These encapsulating efficiencies (EE) were comparable to those of cationic lipoplexes (siRNA-encapsulated cationic LPs) prepared by conventional methods [21]. The weight ratios of siRNA/LP of both LPs were greater than 10%, which is comparable to those of the clinically-used lipid nanoparticle (LNP)-based technology [14,26]. The LPs composed of DOPC and DOPC/DOPE were negatively charged and approximately 150 nm and 550 nm in diameter, respectively. Due to the fusogenic properties of DOPE [27], the LPs composed of DOPC/DOPE may aggregate during preparation.

Table 3.1 Particle properties of the siRNA-encapsulated LPs prepared using the sequential method. N = 3, mean ± S.D.

Formulation (mol%)	EE[a] (wt%)	siRNA/LP (wt%)	Z-average (nm)	PDI (-)	ζ-potential (mV)
DOPC (100)	76.6 ± 0.6	13.3 ± 1.0	155.0 ± 14.2	0.191 ± 0.095	-11.1 ± 1.2
DOPC/DOPE (50/50)	56.9 ± 2.8	10.1 ± 0.4	547.8 ± 342.0	0.676 ± 0.220	-14.9 ± 2.1

[a] EE, encapsulation efficiency.

Next, the $CaCl_2$ concentration was optimized for siRNA encapsulation to pre-formed neutral LPs. When plasmid DNA was encapsulated into pre-formed neutral LPs, optimal $CaCl_2$ concentration was found between 4 and 8 mM [18]. I hereby examined 1, 4, 8, and 16 mM $CaCl_2$ for the encapsulation of siRNA to the LPs composed of DOPC/DOPE. While 16 mM $CaCl_2$ was slightly ineffective in siRNA encapsulation, lower $CaCl_2$ concentrations showed higher EE (Fig. 3.1). Thus, 4 mM $CaCl_2$ was used for siRNA encapsulation of further experiments. These results demonstrated that the use of ethanol and $CaCl_2$ is promising for the preparation of non-cationic LPs containing siRNA, and led us to investigate various phosphatidylcholine (PC)-based phospholipids to stabilize siRNA-encapsulated LPs.

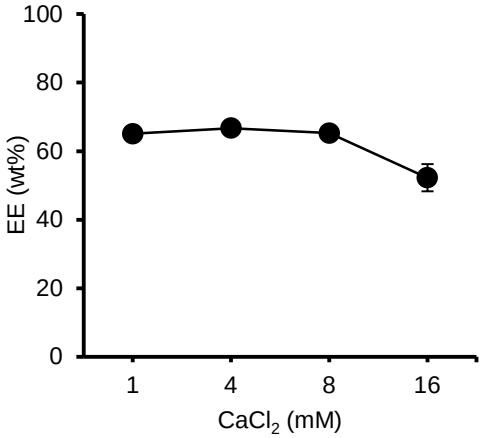

Fig. 3.1 Effect of $CaCl_2$ concentration on the encapsulation efficiency (EE) of LPs composed of DOPC/DOPE. The LPs were prepared by sequential method. N = 3, mean ± S.D.

3.3.2. Effect of phase transition temperature on encapsulation efficiency

When using various types of PC-based phospholipids at 100 mol% (Fig. 3.2A) [28–31], I found that higher phase transition temperatures (T_m) of LPs yielded lower EEs. The correlation plot

between T_m and EE (Fig. 3.2B) indicated that EE was negatively correlated with T_m (R^2 = 0.958), suggesting that the critical factor affecting siRNA encapsulation by this method is the fluidity of the LP lipid membranes.

A

Phosphatidylcholines	T_m (°C)
16:1 (Δ9-cis) PC	-36
DOPC (18:1 (Δ9-Cis) PC)	-18
POPC (16:0-18:1 PC)	-2
18:1 (Δ9-trans) PC	12
DPPC (16:0 PC)	41
DSPC (18:0 PC)	55

B

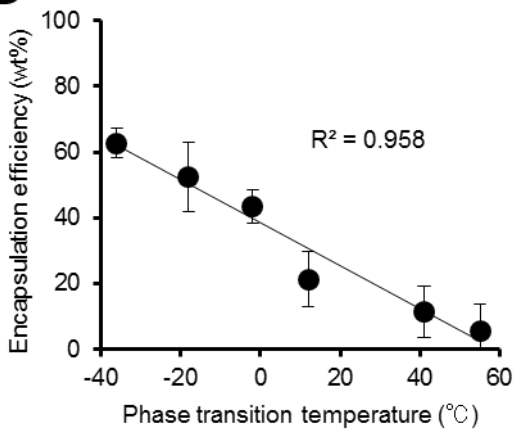

Fig. 3.2 Encapsulation efficiency (EE) of LPs composed of various PC-based phospholipids. (A) Phase transition temperature (T_m) of various PC-based LPs. (B) Relationship between T_m and EE. The LPs were prepared by sequential method. N = 3, mean ± S.D.

3.3.3. Simultaneous method of siRNA encapsulation

Since the sequential method requires pre-formed neutral LPs before encapsulating the siRNA, the complete manufacturing time is relatively long, and harmful organic solvents (chloroform) are frequently used. These issues have prevented large-scale production of siRNA-encapsulated LPs. In contrast, ethanol injection is a simple and rapid method for the preparation of LPs in the absence of other organic solvents [32]. Thus, I have modified the sequential method with ethanol injection. When ethanol-containing phospholipids were instilled into the aqueous solution containing siRNA and $CaCl_2$, I found that siRNA encapsulating LPs were formed (hereafter, referred to as the simultaneous method). As shown in Fig. 3.3A, the EE and weight ratio of siRNA/LP were the same as those of the sequential method (Table 3.1). It was reported that the calcium ion could condense nucleic acids and mediate a bridge between lipid membrane and nucleic acids [33]. Furthermore, ethanol reduced the required concentration of calcium ions required to condense the nucleic acids [18]. The ethanol also enhanced lipid membrane permeability [34]. Thus, the calcium ions and ethanol synergistically enhanced the encapsulation of siRNA into LPs. Surprisingly, the size of the LPs composed of DOPC/DOPE was drastically improved from the aggregated form (diameter: > 500 nm; PDI: ~0.7) to the monodispersed form (diameter: ~200 nm; PDI: ~0.2) (Fig. 3.3B, C), which can be used as a nanocarrier for the drug delivery system (DDS) without size trimming by extrusion. Taken together, I have successfully

eliminated the time-consuming and harmful LP preparation step, and then established the one-step and scalable method to prepare siRNA-encapsulated non-cationic LPs.

A

Formulation (mol)	EE (wt%)	siRNA/LP (wt%)
DOPC (100)	83.6 ± 1.0	11.8 ± 1.0
DOPC/DOPE (50/50)	70.7 ± 0.9	10.9 ± 0.1

N = 3, ± SD

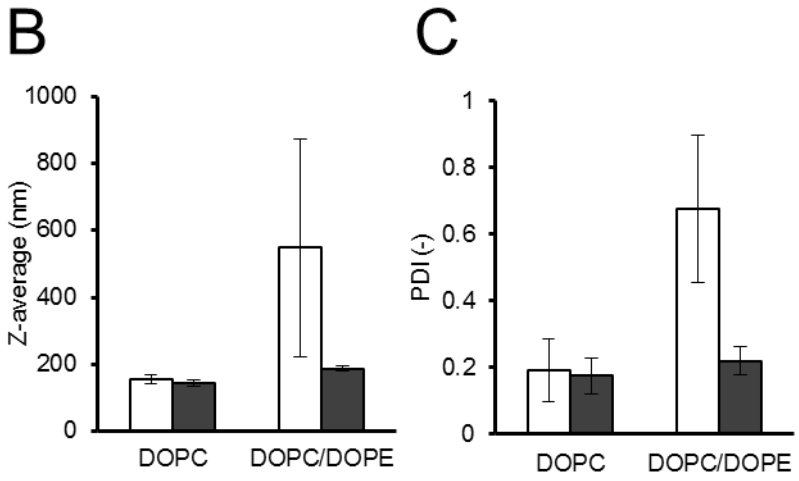

Fig. 3.3 Encapsulation of siRNA into LPs using the simultaneous method. (A) Encapsulation efficiency (EE) and the weight ratio of siRNA/LPs. (B) Z-average and (C) PDI of siRNA-encapsulated LPs (black bars). Control, sequential method (white bars). N = 3, mean ± S.D.

3.3.4. siRNA encapsulation into neutral LPs with high-phase transition temperature

Due to high stability and payload retention, LPs composed of high T_m (> 37°C) PCs are widely used for *in vivo* DDS applications [35]. However, PC-based high T_m LPs cannot encapsulate siRNAs (Fig. 3.2B), strongly suggesting that membrane fluidity is critical for EE. To improve the membrane fluidity of PC-based high T_m LPs, I added up to 40 mol% cholesterol to the LP formulation to act as a fluidity buffer either by disordering the gel state or by ordering the liquid state of the lipids [36]. As shown in Table 3.2, 40 mol% cholesterol drastically improved both the EE (> 60 wt%) and weight ratio of siRNA/LP (> 3 wt%) in the sequential and simultaneous methods. To

prove that the siRNA was encapsulated in the LPs, three types of siRNA-encapsulated LPs (DOPC, DOPC/DOPE, and DPPC/cholesterol) were subjected to FBS treatment (containing RNase and complements; at 37°C for 30 min), and analyzed by agarose gel electrophoresis (Fig. 4). While bare siRNA was completely degraded, the siRNA-encapsulated LPs were protected partially. Based on the densitometric intensity of each band, 92.7, 58.1, and 24.6 wt% of the siRNA in the LPs composed of DOPC, DOPC/DOPE, and DPPC/cholesterol, respectively, were protected from RNase degradation. These results demonstrated that siRNA was less susceptible to RNase after LP encapsulation, suggesting that siRNA-encapsulated non-cationic LPs could remain in circulation for longer times than bare siRNA.

Table 3.2 Particle properties of siRNA-encapsulated LPs composed of DPPC and cholesterol prepared using the sequential and simultaneous method. N = 3, mean ± S.D.

Formulation	Methods	Cholesterol (mol%)	EE[a] (wt%)	siRNA/LP (wt%)	Z-average (nm)
DPPC/ cholesterol	Sequential method	0	0	0	> 1000
		20	0	0	> 1000
		40	64.7 ± 1.3	3.0 ± 0.2	332.7 ± 25.6
	Simultaneous method	0	0	0	> 1000
		20	0	0	> 1000
		40	75.4 ± 3.0	6.9 ± 0.9	257.5 ± 4.4

[a] EE, encapsulation efficiency.

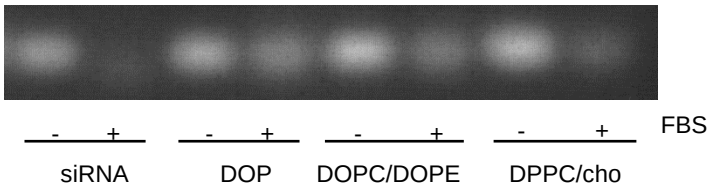

Fig. 3.4 Agarose gel electrophoresis of siRNA-encapsulated LPs. siRNA (100 ng) was encapsulated into LPs (DOPC, DOPC/DOPE [50/50, mol/mol], and DPPC/cholesterol [60/40, mol/mol]) using the simultaneous method, treated with FBS at 37°C for 30 min, and electrophoresed in 2% agarose gel.

3.3.5. siRNA encapsulation into anionic LPs

Compared with neutral LPs, anionic LPs are thought to be more favorable, because they are highly dispersible due to their anionic charge, stable, and retain their payloads. Furthermore, they can circumvent non-specific interactions with cells or proteins *in vivo* because of their negative charge. Thus, anionic LPs may be an ideal nanocarrier for siRNAs. However, the electrostatic repulsion between anionic LPs and siRNA could interfere with siRNA encapsulation. As reported by Asai *et al*. [20] and Negishi *et al*. [37], cholesterol-conjugated siRNA [38] could be inserted into the phospholipid cavity in LPs, and thereby improve the stability of the siRNA-encapsulated LPs. In this study, I attempted to encapsulate cholesterol-conjugated siRNA into anionic LPs (DPPC/DPPE/DPPG-Na/cholesterol, 15/15/30/40 [mol/mol/mol/mol]). As shown in Table 3.3, 37 wt% of siRNA was encapsulated into anionic LPs, and the weight ratio of siRNA/LP was ~5 wt%, whereas the unconjugated siRNA was not encapsulated. The anionic LPs containing cholesterol-conjugated siRNA were ~170 nm in diameter, highly monodispersed (PDI, 0.039), and negatively charged. These particle properties might be suited for *in vivo* systemic siRNA delivery.

Table 3.3 Particle properties of anionic LPs containing unconjugated and cholesterol-conjugated siRNAs. N = 3, mean ± S.D.

Formulation (mol%)	**siRNA**	**EE[a] (wt%)**	**siRNA/LP (wt%)**	**Z-average (nm)**	**PDI (-)**	**ζ-potential (mV)**
DPPC/DPPE/ DPPG-Na/ cholesterol (15/15/30/40)	siRNA	0	0	160.4 ± 3.0	0.033 ± 0.018	-56.7 ± 6.4
	Cholesterol-siRNA	36.5 ± 6.1	4.7 ± 1.1	172.7 ± 5.3	0.039 ± 0.043	-59.2 ± 2.5

[a] EE, encapsulation efficiency.

3.3.6. Cytotoxicity of siRNA-encapsulated LPs

Cationic LPs were widely used for siRNA delivery *in vitro* and *in vivo* [7]; however, cytotoxicity due to the cationic charge remains a problem [8]. Therefore, the *in vitro* cytotoxicity of each siRNA-encapsulated LP (DOPC and DPPC/DPPE/DPPG-Na/cholesterol) was evaluated using HepG2 cells. As a control, cationic lipids (DC-6-14/DOPE/cholesterol) were used (Fig. 3.5) [39]. Non-cationic LPs showed no cytotoxicity at 50 μg/ml, while cationic LPs showed significant cytotoxicity at lower concentrations. The half maximal (50%) inhibitory concentration (IC_{50}) values

of the non-cationic LPs were estimated to be 10-fold higher than that of cationic LPs. Thus, siRNA-encapsulated non-cationic LPs prepared by our method are safer for *in vitro* and *in vivo* siRNA delivery than cationic LPs.

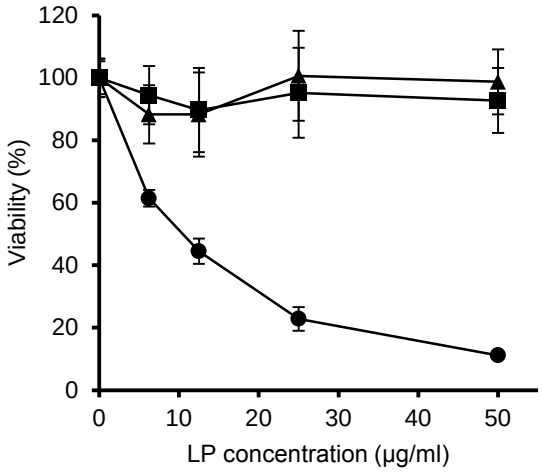

Fig. 3.5 Cytotoxicity of siRNA-encapsulated LPs *in vitro*. HepG2 cells were treated with the indicated concentration of LPs, cultured for 24 h, and then subjected to the WST-8 assay. Both siRNA-encapsulated LPs composed of DOPC (triangles) and DPPC/DPPE/DPPG-Na/cholesterol (squares) were prepared by simultaneous method. LPs composed of DC-6-14/DOPE/cholesterol (circles) were used to prepare lipoplexes by mixing with siRNA (LP/siRNA = 10/1 (wt)). The cell viability of HepG2 cells with no LPs was defined as 100%. N = 8, mean ± S.D.

3.3.7. Targeted delivery of siRNA with non-cationic LPs

Since non-cationic LPs *per se* don't adsorb onto cells *in vitro*, the siRNA-encapsulated non-cationic LPs could not introduce siRNA into cells. Meanwhile, HBV envelop L protein particles produced in yeast cells (bio-nanocapsules, BNCs) [40] have been shown to form a complex with LPs spontaneously and thereby deliver various materials (genes and drugs) *in vitro* and *in vivo* in a human hepatic cells-specific manner [24]. Therefore, anti-firefly luciferase gene siRNA (GL3Luc siRNA) was encapsulated into anionic LPs by simultaneous method, mixed with BNCs to form BNC-LP-siRNA complexes (Z-average, 136.0 ± 18.0 nm; PDI, 0088 ± 0.012; ζ-potential, -37.8 ± 7.5 mV), and then used to transfect Huh7 cells (human hepatic cell-derived cells; target cells for BNC) expressing firefly luciferase. As shown in Fig. 3.6A, BNC-LP-siRNA complexes could suppress the expression of luciferase gene in Huh7 cells by ~50%, while siRNA-encapsulated LP itself could not. Next, I assessed the intracellular localization of siRNA delivered by BNC-LP complexes in Huh7 cells. As a model of siRNA, dsDNA corresponding to GL3Luc siRNA sequence was labeled with 6-FAM and cholesterol (FAM-chol-dsDNA), and encapsulated into anionic LPs by simultaneous method. The complexes were conjugated with BNCs and contacted with Huh7 cells, followed by the

observation under confocal laser scanning microscope (Fig. 3.6B). While LPs could rarely introduce FAM-chol-dsDNA into Huh7 cells, both BNC-LP complexes and positive control could introduce FAM-chol-dsDNA efficiently. The FAM-chol-dsDNA of BNC-LP complexes was partly excluded from late endosomes and lysosomes, and localized as dispersed form in cytoplasm. The results obtained from both experiments indicated that siRNA-encapsulated non-cationic LPs could deploy targeting molecules on the surface, introduce siRNA into the cytoplasm of target cells *in vitro*, and then suppress target genes.

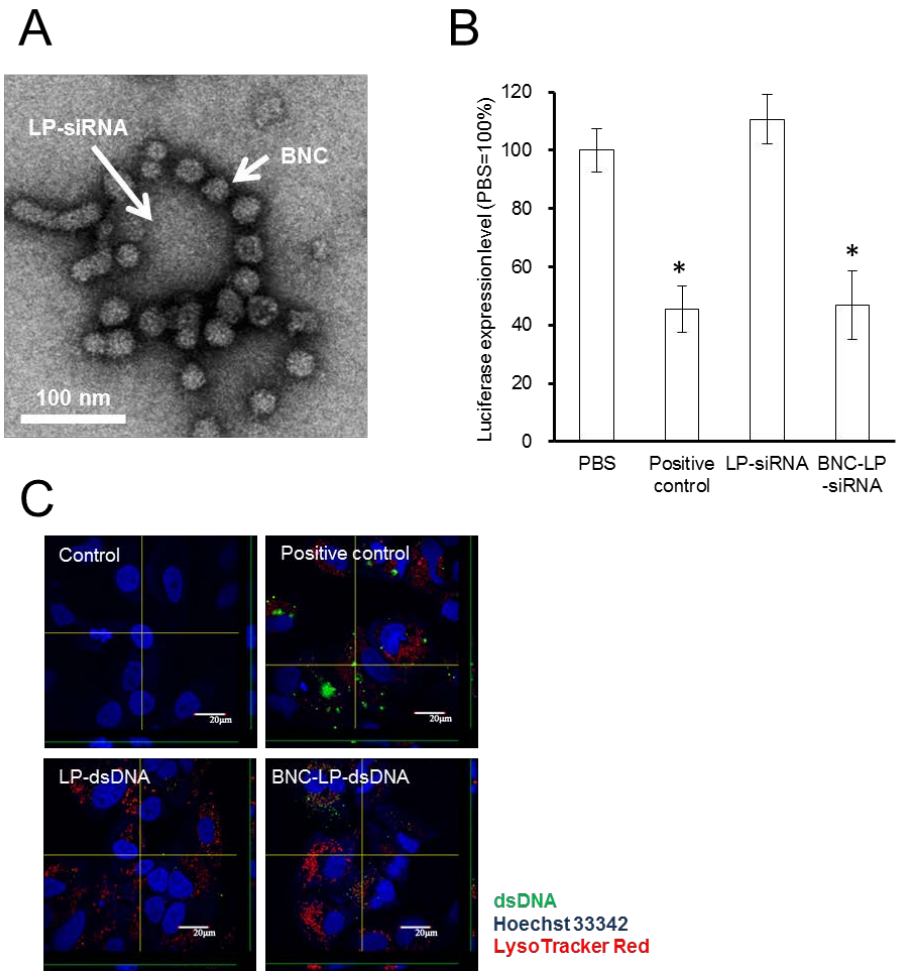

Fig. 3.6 Transfection with BNC-LP-siRNA complexes. (A) Transmission electron micrograph of BNC-LP complexes. (B) Luciferase activities of Huh7 cells transfected with BNC-LP-siRNA complexes, LP-siRNA complexes, and positive control. Luciferase activity in non-treated cells (PBS) was set as 100%. N = 3, mean ± S.D. * indicates $P < 0.01$ by Student's t-test. (C) Intracellular localization of FAM-chol-dsDNA in Huh7 cells. Huh7 cells transfected with BNC-LP-siRNA complexes, LP-siRNA complexes, and positive control were observed under confocal laser scanning

microscope. FAM-chol-dsDNA, green; LysoTracker Red, red; and Hoechst 33342(nuclei marker), blue. Bars, 20 μm.

3.3.8. Encapsulation of siRNA into PEGylated non-cationic LPs

For the *in vivo* application of siRNA-encapsulated non-cationic LPs, it was examined whether polyethylene glycol (PEG)-conjugated phospholipids are applicable to the simultaneous method. Various ratios of DOPE-PEG2000 (from 0 to 5 mol% of total lipids) were mixed with DOPC and then formulated to siRNA-encapsulated LPs. All siRNA-encapsulated PEGylated LPs showed comparable level of EE (approx. 60 wt%), while non-PEGylated LPs showed EE of approx. 70 wt% (Fig. 7), indicating that PEG moiety did not always impede siRNA encapsulation. The size and weight ratios of siRNA/LP of siRNA-encapsulated PEGylated LPs were 100 ~ 130 nm in diameters and approx. 7 wt%, respectively. Thus, siRNA-encapsulated non-cationic LPs could be PEGylated for the *in vivo* systemic siRNA delivery.

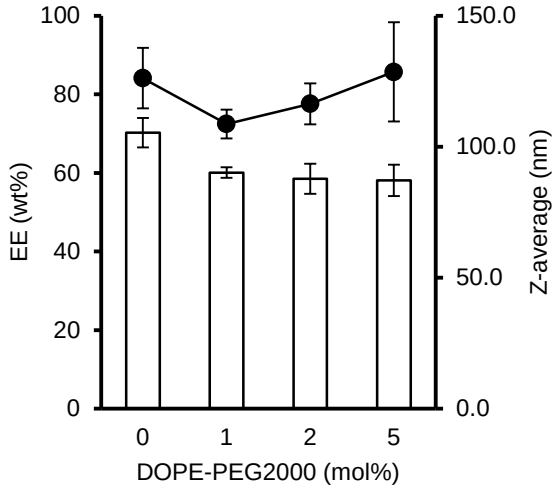

Fig. 7. Effect of DOPE-PEG2000 on the EE and Z-average of siRNA-encapsulated LPs composed of DOPC. Bars, EE; and circles, Z-average. N = 3, mean ± S.D.

3.4. Conclusion

In this study, I established a one-step and scalable method (simultaneous method) to prepare neutral LPs with high siRNA levels, which utilized ethanol injection and siRNA condensation by calcium ion. In particular, I have succeeded in encapsulating substantial amounts of siRNA into anionic LPs using cholesterol-conjugated siRNA. Our method would be applicable not only to siRNA, but also to other nucleic acid therapeutics, such as microRNAs or antisense nucleic acids. By arming with the machineries for targeting cells, enhancing cellular uptake, and endosomal escape on the surface of LPs, these LPs could be an alternative to conventional cationic LP-based siRNA delivery systems.

3.5. References

[1] M.R. Lares, J.J. Rossi, D.L. Ouellet, RNAi and small interfering RNAs in human disease therapeutic applications., Trends Biotechnol. 28 (2010) 570–9. doi:10.1016/j.tibtech.2010.07.009.

[2] Y. Matsumura, H. Maeda, A new concept for macromolecular therapeutics in cnacer chemotherapy: mechanism of tumoritropic accumulatio of proteins and the antitumor agents Smancs, Cancer Res. 46 (1986) 6387– 6392. http://cancerres.aacrjournals.org/content/46/12_Part_1/6387.short (accessed January 22, 2015).

[3] S. Gao, F. Dagnaes-Hansen, E.J.B. Nielsen, J. Wengel, F. Besenbacher, K.A. Howard, et al., The effect of chemical modification and nanoparticle formulation on stability and biodistribution of siRNA in mice., Mol. Ther. 17 (2009) 1225–33. doi:10.1038/mt.2009.91.

[4] R. Kanasty, J.R. Dorkin, A. Vegas, D. Anderson, Delivery materials for siRNA therapeutics., Nat. Mater. 12 (2013) 967–77. doi:10.1038/nmat3765.

[5] P. Resnier, T. Montier, V. Mathieu, J.-P. Benoit, C. Passirani, A review of the current status of siRNA nanomedicines in the treatment of cancer., Biomaterials. 34 (2013) 6429–43. doi:10.1016/j.biomaterials.2013.04.060.

[6] J.-H. Kang, Y. Tachibana, W. Kamata, A. Mahara, M. Harada-Shiba, T. Yamaoka, Liver-targeted siRNA delivery by polyethylenimine (PEI)-pullulan carrier., Bioorg. Med. Chem. 18 (2010) 3946–50. doi:10.1016/j.bmc.2010.04.031.

[7] A. Sato, M. Takagi, A. Shimamoto, S. Kawakami, M. Hashida, Small interfering RNA delivery to the liver by intravenous administration of galactosylated cationic liposomes in mice., Biomaterials. 28 (2007) 1434–42. doi:10.1016/j.biomaterials.2006.11.010.

[8] H. Lv, S. Zhang, B. Wang, S. Cui, J. Yan, Toxicity of cationic lipids and cationic polymers in gene delivery., J. Control. Release. 114 (2006) 100–9. doi:10.1016/j.jconrel.2006.04.014.

[9] J.P. Yang, L. Huang, Overcoming the inhibitory effect of serum on lipofection by increasing the charge ratio of cationic liposome to DNA., Gene Ther. 4 (1997) 950–60. doi:10.1038/sj.gt.3300485.

[10] Y. Omidi, A.J. Hollins, M. Benboubetra, R. Drayton, I.F. Benter, S. Akhtar, Toxicogenomics of non-viral vectors for gene therapy: a microarray study of lipofectin- and oligofectamine-induced gene expression changes in human epithelial cells., J. Drug Target. 11 (2003) 311–23. doi:10.1080/10611860310001636908.

[11] M. Kapoor, D.J. Burgess, Efficient and safe delivery of siRNA using anionic lipids: Formulation optimization studies., Int. J. Pharm. 432 (2012) 80–90. doi:10.1016/j.ijpharm.2012.04.058.

[12] M. Ukawa, H. Akita, Y. Hayashi, R. Ishiba, K. Tange, M. Arai, et al., Neutralized Nanoparticle Composed of SS-Cleavable and pH-Activated Lipid-Like Material as a Long-Lasting and

Liver-Specific Gene Delivery System., Adv. Healthc. Mater. 3 (2014) 1–8. doi:10.1002/adhm.201300629.

[13] S.C. Semple, S.K. Klimuk, T.O. Harasym, N. Dos Santos, S.M. Ansell, K.F. Wong, et al., Efficient encapsulation of antisense oligonucleotides in lipid vesicles using ionizable aminolipids: formation of novel small multilamellar vesicle structures, Biochim. Biophys. Acta - Biomembr. 1510 (2001) 152–166. doi:10.1016/S0005-2736(00)00343-6.

[14] A. Akinc, W. Querbes, S. De, J. Qin, M. Frank-Kamenetsky, K.N. Jayaprakash, et al., Targeted delivery of RNAi therapeutics with endogenous and exogenous ligand-based mechanisms., Mol. Ther. 18 (2010) 1357–64. doi:10.1038/mt.2010.85.

[15] T. Coelho, D. Adams, A. Silva, P. Lozeron, P.N. Hawkins, T. Mant, et al., Safety and efficacy of RNAi therapy for transthyretin amyloidosis., N. Engl. J. Med. 369 (2013) 819–29. doi:10.1056/NEJMoa1208760.

[16] M. Kapoor, D.J. Burgess, Physicochemical characterization of anionic lipid-based ternary siRNA complexes., Biochim. Biophys. Acta. 1818 (2012) 1603–1612. doi:10.1016/j.bbamem.2012.03.013.

[17] C.N. Landen, A. Chavez-Reyes, C. Bucana, R. Schmandt, M.T. Deavers, G. Lopez-Berestein, et al., Therapeutic EphA2 gene targeting in vivo using neutral liposomal small interfering RNA delivery, Cancer Res. 65 (2005) 6910–6918. doi:10.1158/0008-5472.CAN-05-0530.

[18] A.L. Bailey, S.M. Sullivan, Efficient encapsulation of DNA plasmids in small neutral liposomes induced by ethanol and calcium, Biochim. Biophys. Acta - Biomembr. 1468 (2000) 239–252. doi:10.1016/S0005-2736(00)00264-9.

[19] S.M. Elbashir, J. Harborth, K. Weber, T. Tuschl, Analysis of gene function in somatic mammalian cells using small interfering RNAs., Methods. 26 (2002) 199–213. doi:10.1016/S1046-2023(02)00023-3.

[20] T. Asai, S. Matsushita, E. Kenjo, T. Tsuzuku, N. Yonenaga, H. Koide, et al., Dicetyl phosphate-tetraethylenepentamine-based liposomes for systemic siRNA delivery., Bioconjug. Chem. 22 (2011) 429–35. doi:10.1021/bc1004697.

[21] J. Heyes, L. Palmer, K. Bremner, I. MacLachlan, Cationic lipid saturation influences intracellular delivery of encapsulated nucleic acids., J. Control. Release. 107 (2005) 276–87. doi:10.1016/j.jconrel.2005.06.014.

[22] S. Kuroda, S. Otaka, T. Miyazaki, M. Nakao, Y. Fujisawa, Hepatitis B virus envelope L protein particles: Synthesis and assembly in Saccharomyces cerevisiae, purification and characterization, J. Biol. Chem. 267 (1992) 1953–1961. http://www.ncbi.nlm.nih.gov/pubmed/18434744.

[23] J. Jung, M. Iijima, N. Yoshimoto, M. Sasaki, T. Niimi, K. Tatematsu, et al., Efficient and rapid purification of drug- and gene-carrying bio-nanocapsules, hepatitis B virus surface antigen L

particles, from Saccharomyces cerevisiae., Protein Expr. Purif. 78 (2011) 149–55. doi:10.1016/j.pep.2011.04.008.

[24] J. Jung, T. Matsuzaki, K. Tatematsu, T. Okajima, K. Tanizawa, S. Kuroda, Bio-nanocapsule conjugated with liposomes for in vivo pinpoint delivery of various materials., J. Control. Release. 126 (2008) 255–64. doi:10.1016/j.jconrel.2007.12.002.

[25] H.T.S. Britton, R.A. Robinson, CXCVIII. Universal Buger Solutions and the Dissociation Constant of Veronal, J. Chem. Soc. (1923) 1456–1462. doi:10.1039/JR9310001456.

[26] J. Gilleron, W. Querbes, A. Zeigerer, A. Borodovsky, G. Marsico, U. Schubert, et al., Image-based analysis of lipid nanoparticle-mediated siRNA delivery, intracellular trafficking and endosomal escape., Nat. Biotechnol. 31 (2013) 638–46. doi:10.1038/nbt.2612.

[27] H.R. Marsden, I. Tomatsu, A. Kros, Model systems for membrane fusion., Chem. Soc. Rev. 40 (2011) 1572–85. doi:10.1039/c0cs00115e.

[28] R. Koynova, M. Caffrey, Phases and phase transitions of the phosphatidylcholines, Biochim. Biophys. Acta - Rev. Biomembr. 1376 (1998) 91–145. doi:10.1016/S0304-4157(98)00006-9.

[29] S. Leekumjorn, A.K. Sum, Molecular characterization of gel and liquid-crystalline structures of fully hydrated POPC and POPE bilayers., J. Phys. Chem. B. 111 (2007) 6026–33. doi:10.1021/jp0686339.

[30] S. Mabrey, J.M. Sturtevant, Investigation of phase transitions of lipids and lipid mixtures by sensitivity differential scanning calorimetry., Proc. Natl. Acad. Sci. 73 (1976) 3862–3866. doi:10.1073/pnas.73.11.3862.

[31] P.W.M. Van Dijck, B. De Kruijff, L.L.M. Van Deenen, J. De Gier, R. a. Demel, The preference of cholesterol for phosphatidylcholine in mixed phosphatidylcholine-phosphatidylethanolamine bilayers, Biochim. Biophys. Acta - Biomembr. 455 (1976) 576–587. doi:10.1016/0005-2736(76)90326-6.

[32] S. Batzri, E.D. Korn, Single bilayer liposomes prepared without sonication, Biochim. Biophys. Acta - Biomembr. 298 (1973) 1015–1019. doi:10.1016/0005-2736(73)90408-2.

[33] S.D. Patil, D.G. Rhodes, D.J. Burgess, Anionic liposomal delivery system for DNA transfection., AAPS J. 6 (2004) e29. doi:10.1208/aapsj060429.

[34] H. Komatsu, S. Okada, Increased permeability of phase-separated liposomal membranes with mixtures of ethanol-induced interdigitated and non-interdigitated structures., Biochim. Biophys. Acta. 1237 (1995) 169–175. doi:10.1016/0005-2736(95)00098-N.

[35] D.C. Drummond, O. Meyer, K. Hong, D.B. Kirpotin, D. Papahadjopoulos, Optimizing liposomes for delivery of chemotherapeutic agents to solid tumors., Pharmacol. Rev. 51 (1999) 691–743. doi:VL - 51.

[36] C. Chen, D. Han, C. Cai, X. Tang, An overview of liposome lyophilization and its future potential., J. Control. Release. 142 (2010) 299–311. doi:10.1016/j.jconrel.2009.10.024.

[37] Y. Negishi, Y. Endo-Takahashi, K. Ishii, R. Suzuki, Y. Oguri, T. Murakami, et al., Development of novel nucleic acid-loaded Bubble liposomes using cholesterol-conjugated siRNA, J. Drug Target. 19 (2011) 830–836. doi:10.3109/1061186X.2011.585428.

[38] J. Soutschek, A. Akinc, B. Bramlage, K. Charisse, R. Constien, M. Donoghue, et al., Therapeutic silencing of an endogenous gene by systemic administration of modified siRNAs., Nature. 432 (2004) 173–8. doi:10.1038/nature03121.

[39] A. Kikuchi, Y. Aoki, S. Sugaya, T. Serikawa, K. Takakuwa, K. Tanaka, et al., Development of novel cationic liposomes for efficient gene transfer into peritoneal disseminated tumor., Hum. Gene Ther. 10 (1999) 947–55. doi:10.1089/10430349950018346.

[40] T. Yamada, Y. Iwasaki, H. Tada, H. Iwabuki, M.K.L. Chuah, T. VandenDriessche, et al., Nanoparticles for the delivery of genes and drugs to human hepatocytes., Nat. Biotechnol. 21 (2003) 885–890. doi:10.1038/nbt843.

Chapter IV Comprehensive discussion

4.1. Comprehensive discussion

In this study, I established cytoplasmic siRNA delivery system by utilizing human hepatocyte-specific nanocarrier, BNC-LP complexes. To date, several research groups have developed HBV-inspired DDS nanocarriers, such as pre-S1-displaying forms of protein nanocages [1,2], LPs [3–5], and polymer micelles [6]. These studies are based on the fact that pre-S1 domain of L protein plays a crucial role in the hepatocyte-recognition of HBV [7–9]. As described in Chapter III, sodium taurocholate cotransporting polypeptide (NTCP) was recently identified as a functional receptor of HBV [10]. Furthermore, N-terminal approx. 50 aa of pre-S1 region was shown to interact with NTCP [11], while HBV requires both pre-S1 and S region to infect with human hepatocyte [12]. In addition to the NTCP binding function of pre-S1, heparan sulfate proteoglycan (HSPG)-mediated binding is prerequisite for the early infection of HBV [13–15]. The antigenic loop in S region is required to interact with HSPG [16,17]. Thus, the involvement of at least two parts, N-terminal approx. 50 aa of pre-S1 region and antigenic loop of S region, is postulated to reconstitute the HBV infection machinery in synthetic nanocarriers. Since BNC harbors full-length L protein including pre-S1, pre-S2, and S region, and deploys whole pre-S1 region and antigenic loop of S region outwardly, BNC can exploit the HBV infection machinery by utilizing both HSPG- and NTCP-mediated binding. In the previous study, BNC was reported to interact with human hepatic cells through cell-surface proteoglycan [18]. Thus, in the future, it should be addressed whether NTCP could interact with BNC and mediate cell entry or intracellular trafficking of BNC.

As described in Chapter II, BNC was found to fuse with lipid bilayer by the short peptide sequence (9-24 aa of pre-S1 region) in a low pH-dependent manner, which contains fusogenic domain and thereby plays a crucial role in membrane fusion, membrane disruption, and payload release of BNC-LP complexes. These findings are important not only for the application of BNC-LP complexes as DDS nanocarriers, but also for the understanding of life cycle of HBV (especially in the early infection machinery). Membrane fusion and subsequent uncoating process of natural HBV are still unsettled [19]. Although I identified fusogenic domain in the pre-S1 region of L protein, it is still unknown whether HBV utilizes the fusogenic domain for its entry into human hepatocyte. I anticipate that BNC could be a useful tool to fully understand how HBV enters into cells, fuses with host membrane, and releases its contents to cytoplasm.

As for the fusogenic domain of pre-S1 region, low pH condition was shown to induce conformational change of at least pre-S1 region (*see* Figs. 2.2C & D), which might be mediated by the neutralization of two negatively charged aspartic acid residues within 9-24 aa of pre-S1 (D16 and D20). In other viruses, low pH-induced conformational change is important for the membrane fusion in acidic environment, and several negatively charged amino acid residues play a critical role in the

membrane fusion. In case of Semliki Forest virus (SFV), neutralization of aspartic acid residue (D188) in fusion protein E1 is prerequisite for the E1 trimerization, which mediates the initiation of membrane fusion [20]. Another example of low pH-dependent membrane fusion protein is GALA, a synthetic 30-aa peptide designed for the low pH-dependent membrane fusion activity [21]. GALA peptide could interact with lipid bilayer only in the acidic condition, since the acidic glutamic acid residues become neutralized and form amphiphilic α-helix conformation, which initiate membrane fusion. These studies indicated that the acidic amino acid residues (aspartic acid and glutamic acid) in fusion protein are likely to sensor the low pH environment to fuse with lipid bilayer. Although pre-S1 peptide is not likely to form ordered secondary conformation, such as α-helix [22,23], it is possible that neutralization of aspartic acids in low pH could enhance the affinity between pre-S1 fusogenic domain and lipid bilayer or presumably facilitate the stabilization of oligomerized form of L protein. Thus, in the future, two aspartic acid residues in the pre-S1 fusogenic domain should be examined whether they are responsible for the membrane fusion of BNC and HBV presumably in acidic endosome. Furthermore, the fusogenic domain of pre-S1 could be used as a low pH-dependent cell penetrating peptide (CPP). Inspired by virus infection machinery, various types of CPPs have been developed and used for the delivery system of drugs and genes [24,25]. When the pre-S1 fusogenic peptide is decorated on the surface of LPs, they could work for membrane fusion and subsequent endosomal escape in acidic endosome, followed by cytoplasmic delivery of payloads.

In Chapter III, I established a novel one-step method to encapsulate siRNA into non-cationic LPs. Comparing with conventional methods utilizing non-cationic LPs, the encapsulation efficiency and total encapsulated amounts of siRNA were the highest level (~80 wt% and ~10 wt% of LPs, respectively). This method could be applied not only to siRNA, but also to other nucleic acid medicines, such as microRNA, antisense oligonucleotide, and decoy oligonucleotide, etc. As for the siRNA delivery, I succeeded in the targeted delivery of siRNA by BNC-LP complexes (Fig. 3.6); however, knockdown efficiency was still low compared with conventional cationic LPs. When the formulation of BNC-LP complexes is optimized for siRNA delivery, they might be an ideal nanocarrier for *in vivo* siRNA delivery. Lipid composition might be a critical factor for enhancing knockdown activity of non-cationic LPs-mediated siRNA delivery. In case of the LNP formulation, the structure of hydrophobic moiety of lipids significantly affects the knockdown efficiency. For example, Akita *et al.* found that hydrophobic group of SS-cleavable proton-activated lipid-like material (ssPalm), an alternative of ionizable lipids, is critical for siRNA delivery efficiency. When the LNP formulated with ssPalm containing vitamin E as hydrophobic moiety was administrated to mice intravenously, potent knockdown efficiency was observed, while LNP formulated with ssPalm containing myristic acid showed no knockdown effect [26]. This study suggests that hydrophobic moiety of lipids significantly affects the knockdown efficiency of LNP. Another study revealed that the degree of unsaturation of ionizable lipids is critical for knockdown

efficiency of LNP [27]. Fusogenicity and knockdown efficiency of LNP were well correlated with the degree of unsaturation in fatty acid group. Especially, LNP composed of ionizable lipids containing two double bonds showed highest fusogenic activity and knockdown efficiency. According to these studies, by the modification of lipid moiety of BNC-LP complexes, knockdown efficiency might be further improved. In the present study, I utilized DPPC/DPPE/DPPG-Na/cholesterol (15/15/30/40, mol) formulation for LP preparation. These lipids are composed of fully saturated lipids, possessing low fusogenicity and rigid lipid bilayer (T_m = 41~63°C). If the lipid moiety of BNC-LP complexes is replaced with highly fusogenic lipids or unsaturated lipids, both endosomal escape efficiency and knockdown efficiency of BNC-LP complexes would be improved. In addition to the nanocarriers, chemically modified siRNAs by themselves were shown to increase the stability against nuclease and knockdown efficiency, concurrently decrease the immunogenicity of siRNA [28–30]. If BNC-LP complexes are combined with these kinds of modified siRNA, knockdown efficiency might be improved.

Ideally, BNC-LP complex has to be simplified as they are difficult to produce in mass-scale for clinical application. Chemistry, manufacturing, and control (CMC) is the critical factor for mass scale production and quality control for the commercialization of nanomedicines. Due to the usage of recombinant yeast cells for the production of BNC, manufacturing process of BNC-LP complexes is relatively complicated compared with synthetic nanocarriers composed of chemically-defined materials. If the pleiotropic HBV-derived functions, such as human hepatocyte-specific binding ability (binding to both HSPG and NTCP), membrane fusion activity, and stealth activity, are reconstituted by conjugating functional short peptides rationally on the surface of non-cationic LPs, they could be a powerful DDS nanocarrier for siRNA delivery by mimicking infection machinery of HBV.

4.2. References

[1] M. Murata, S. Narahara, K. Umezaki, R. Toita, S. Tabata, J.S. Piao, et al., Liver cell specific targeting by the preS1 domain of hepatitis B virus surface antigen displayed on protein nanocages., Int. J. Nanomedicine. 7 (2012) 4353–62. doi:10.2147/IJN.S31365.

[2] M. Murata, J.S. Piao, S. Narahara, T. Kawano, N. Hamano, J.-H. Kang, et al., Expression and characterization of myristoylated preS1-conjugated nanocages for targeted cell delivery, Protein Expr. Purif. 110 (2015) 52–56. doi:10.1016/j.pep.2014.12.001.

[3] Z. Wang, Z. Yuan, L. Jin, Gene delivery into hepatocytes with the preS/liposome/DNA system., Biotechnol. J. 3 (2008) 1286–95. doi:10.1002/biot.200800125.

[4] X. Zhang, Q. Zhang, Q. Peng, J. Zhou, L. Liao, X. Sun, et al., Hepatitis B virus preS1-derived lipopeptide functionalized liposomes for targeting of hepatic cells., Biomaterials. 35 (2014) 6130–41. doi:10.1016/j.biomaterials.2014.04.037.

[5] Q. Zhang, X. Zhang, T. Chen, X. Wang, Y. Fu, Y. Jin, et al., A safe and efficient hepatocyte-selective carrier system based on myristoylated preS1/21-47 domain of hepatitis B virus., Nanoscale. 7 (2015) 9298–9310. doi:10.1039/c4nr04730c.

[6] R. Miyata, M. Ueda, H. Jinno, T. Konno, K. Ishihara, N. Ando, et al., Selective targeting by preS1 domain of hepatitis B surface antigen conjugated with phosphorylcholine-based amphiphilic block copolymer micelles as a biocompatible, drug delivery carrier for treatment of human hepatocellular carcinoma with paclitaxel, Int. J. Cancer. 124 (2009) 2460–2467. doi:10.1002/ijc.24227.

[7] A.R. Neurath, S.B. Kent, N. Strick, K. Parker, Identification and chemical synthesis of a host cell receptor binding site on hepatitis B virus., Cell. 46 (1986) 429–436. doi:0092-8674(86)90663-X.

[8] P. Gripon, I. Cannie, S. Urban, Efficient Inhibition of Hepatitis B Virus Infection by Acylated Peptides Derived from the Large Viral Surface Protein Efficient Inhibition of Hepatitis B Virus Infection by Acylated Peptides Derived from the Large Viral Surface Protein, J. Virol. 79 (2005) 1613–1622. doi:10.1128/JVI.79.3.1613.

[9] A. Meier, S. Mehrle, T.S. Weiss, W. Mier, S. Urban, Myristoylated PreS1-domain of the hepatitis B virus L-protein mediates specific binding to differentiated hepatocytes., Hepatology. 58 (2013) 31–42. doi:10.1002/hep.26181.

[10] H. Yan, G. Zhong, G. Xu, W. He, Z. Jing, Z. Gao, et al., Sodium taurocholate cotransporting polypeptide is a functional receptor for human hepatitis B and D virus., Elife. 1 (2012) e00049. doi:10.7554/eLife.00049.

[11] K. Watashi, A. Sluder, T. Daito, S. Matsunaga, A. Ryo, S. Nagamori, et al., Cyclosporin A and its analogs inhibit hepatitis B virus entry into cultured hepatocytes through targeting a membrane transporter, sodium taurocholate cotransporting polypeptide (NTCP)., Hepatology. 59 (2014) 1726–37. doi:10.1002/hep.26982.

[12] Y. Le Duff, M. Blanchet, C. Sureau, The pre-S1 and antigenic loop infectivity determinants of the hepatitis B virus envelope proteins are functionally independent., J. Virol. 83 (2009) 12443–12451. doi:10.1128/JVI.01594-09.

[13] C.M. Leistner, S. Gruen-Bernhard, D. Glebe, Role of glycosaminoglycans for binding and infection of hepatitis B virus., Cell. Microbiol. 10 (2008) 122–33. doi:10.1111/j.1462-5822.2007.01023.x.

[14] E.R. Verrier, C.C. Colpitts, C. Bach, L. Heydmann, A. Weiss, G. Abou-jaoudé, et al., A targeted functional RNAi screen uncovers Glypican 5 as an entry factor for hepatitis B and D viruses List of Abbreviations, (2015) 1–44. doi:10.1002/hep.28013.

[15] S. Urban, Entry and entry inhibition of Hepatitis B (HBV) and Hepatitis Delta Virus (HDV) into hepatocytes, Hepatology. (2015) n/a–n/a. doi:10.1002/hep.28308.

[16] J. Salisse, C. Sureau, A function essential to viral entry underlies the hepatitis B virus “a” determinant., J. Virol. 83 (2009) 9321–9328. doi:10.1128/JVI.00678-09.

[17] C. Sureau, J. Salisse, A conformational heparan sulfate binding site essential to infectivity overlaps with the conserved hepatitis B virus A-determinant, Hepatology. 57 (2013) 985–994. doi:10.1002/hep.26125.

[18] T. Kasuya, S. Nomura, T. Matsuzaki, J. Jung, T. Yamada, K. Tatematsu, et al., Expression of squamous cell carcinoma antigen-1 in liver enhances the uptake of hepatitis B virus envelope-derived bio-nanocapsules in transgenic rats., FEBS J. 275 (2008) 5714–24. doi:10.1111/j.1742-4658.2008.06698.x.

[19] K. Watashi, S. Urban, W. Li, T. Wakita, NTCP and beyond: opening the door to unveil hepatitis B virus entry., Int. J. Mol. Sci. 15 (2014) 2892–905. doi:10.3390/ijms15022892.

[20] C.Y. Liu, M. Kielian, E1 mutants identify a critical region in the trimer interface of the Semliki forest virus fusion protein., J. Virol. 83 (2009) 11298–11306. doi:10.1128/JVI.01147-09.

[21] R. a. Parente, S. Nir, F.C. Szoka, pH-dependent fusion of phosphatidylcholine small vesicles. Induction by a synthetic amphipathic peptide, J. Biol. Chem. 263 (1988) 4724–4730.

[22] S. De Falco, M. Ruvo, a Verdoliva, a Scarallo, D. Raimondo, a Raucci, et al., N-terminal myristylation of HBV preS1 domain enhances receptor recognition., J. Pept. Res. 57 (2001) 390–400. doi:jpr848 [pii].

[23] E. Núñez, X. Wei, C. Delgado, I. Rodríguez-Crespo, B. Yélamos, J. Gómez-Gutiérrez, et al., Cloning, expression, and purification of histidine-tagged preS domains of hepatitis B virus., Protein Expr. Purif. 21 (2001) 183–91. doi:10.1006/prep.2000.1368.

[24] B. Gupta, T.S. Levchenko, V.P. Torchilin, Intracellular delivery of large molecules and small particles by cell-penetrating proteins and peptides., Adv. Drug Deliv. Rev. 57 (2005) 637–51. doi:10.1016/j.addr.2004.10.007.

[25] S. Trabulo, A.L. Cardoso, M. Mano, M.C.P. de Lima, Cell-Penetrating Peptides—Mechanisms of Cellular Uptake and Generation of Delivery Systems, Pharmaceuticals. 3 (2010) 961–993. doi:10.3390/ph3040961.

[26] H. Akita, Y. Noguchi, H. Hatakeyama, Y. Sato, K. Tange, Y. Nakai, et al., Molecular Tuning of a Vitamin E-Scaffold pH-Sensitive and Reductive Cleavable Lipid-like Material for Accelerated in Vivo Hepatic siRNA Delivery, ACS Biomater. Sci. Eng. 1 (2015) 834–844. doi:10.1021/acsbiomaterials.5b00203.

[27] J. Heyes, L. Palmer, K. Bremner, I. MacLachlan, Cationic lipid saturation influences intracellular delivery of encapsulated nucleic acids., J. Control. Release. 107 (2005) 276–87. doi:10.1016/j.jconrel.2005.06.014.

[28] A.D. Judge, G. Bola, A.C.H. Lee, I. MacLachlan, Design of noninflammatory synthetic siRNA mediating potent gene silencing in vivo, Mol. Ther. 13 (2006) 494–505. doi:10.1016/j.ymthe.2005.11.002.

[29] Y. Chiu, T.M. Rana, siRNA function in RNAi: a chemical modification analysis., RNA. 9 (2003) 1034–1048. doi:10.1261/rna.5103703.

[30] S.Y. Wu, X. Yang, K.M. Gharpure, H. Hatakeyama, M. Egli, M.H. McGuire, et al., 2'-OMe-phosphorodithioate-modified siRNAs show increased loading into the RISC complex and enhanced anti-tumour activity., Nat. Commun. 5 (2014) 3459. doi:10.1038/ncomms4459.

List of publications

Publications for dissertation

1. M. Somiya, Y. Sasaki, T. Matsuzaki, Q. Liu, M. Iijima, N. Yoshimoto, T. Niimi, A. D. Maturana, and S. Kuroda, “Intracellular trafficking of bio-nanocapsule–liposome complex: Identification of fusogenic activity in the pre-S1 region of hepatitis B virus surface antigen L protein,” *Journal of Controlled Release*. vol. 212, pp. 10–18, Aug. 2015.
2. M. Somiya, K. Yamaguchi, Q. Liu, T. Niimi, A. D. Maturana, M. Iijima, N. Yoshimoto, and S. Kuroda, “One-step scalable preparation method for non-cationic liposomes with high siRNA content,” *International Journal of Pharmaceutics*, vol. 490, no. 1–2, pp. 316–323, 2015.

Other publications

Original papers

1. M. Somiya, N. Yoshimoto, M. Iijima, T. Niimi, T. Dewa, J. Jung, and S. Kuroda, “Targeting of polyplex to human hepatic cells by bio-nanocapsules, hepatitis B virus surface antigen L protein particles” *Bioorganic Medicinal Chemistry*, vol. 20, no. 12, pp. 3873–9, Jun. 2012.
2. M. Iijima, M. Somiya, N. Yoshimoto, T. Niimi, and S. Kuroda, “Nano-visualization of oriented-immobilized IgGs on immunosensors by high-speed atomic force microscopy” *Scientific Reports*, vol. 2, p. 790, Jan. 2012.
3. Q. Liu, J. Jung, M. Somiya, M. Iijima, N. Yoshimoto, Tomoaki Niimi, A. D. Maturana, S. H. Shin, S.-Y. Jeong, E. K. Choi, and S. Kuroda, “Virosomes of hepatitis B virus envelope L proteins containing doxorubicin: synergistic enhancement of human liver-specific antitumor growth activity by radiotherapy,” *International Journal of Nanomedicine*, p. 4159, Jun. 2015.

Reviews

1. M Somiya, N Yoshimoto, and S Kuroda, “Application of Bionanocapsule-liposome complex for in vivo pinpoint drug delivery” *Monthly Fine Chemical* (written in Japanese), Volume 42, No 4, April, 2013
2. M Somiya and S Kuroda, “Development of a Virus-mimicking Nanocarrier for Drug Delivery Systems: the Bio-nanocapsule” *Advanced Drug Delivery Reviews*, vol. 95, p. 77, 2016
3. M Somiya and S Kuroda, “Potential of non-cationic liposome-based delivery systems for nucleic acid medicines” *Drug Delivery System*, (written in Japanese) 31-1, 2016

Books

1. M Somiya, K Yamaguchi, and S Kuroda, “Development of bio-nanocapsule-liposome complexes (virosomes) for the cytoplasmic siRNA delivery” *PROGRESS IN DRUG DELIVERY SYSTEM XXIV*, (written in Japanese) 2015

Conferences

International conferences

1. M Somiya, S Kuroda, Enhancement of Active Targeting and Cellular Uptake of Liposomes by Bio-nanocapsule Modification. 2013 Annual Meeting of Controlled Release Society, Hawaii, US (July, 2013), poster presentation
2. M Somiya, K Yamaguchi, and S Kuroda, Targeted Delivery of siRNA into Cytoplasm of Human Hepatic Cells by Bio-nanocapsule-liposome Complex. Liposome Research Days 2014, Copenhagen, Denmark (August, 2014), poster presentation
3. M Somiya, K Yamaguchi, S Kuroda, Efficient One-step Preparation of siRNA-encapsulated Non-cationic Liposomes. 2015 Annual Meeting of Controlled Release Society, Edinburgh, UK (July, 2015), poster presentation
4. M Somiya, S Kuroda, "Role of the pre-S1 fusogenic domain in the early infection machinery of HBV", 2015 International Meeting on Molecular Biology of Hepatitis B Viruses, Bad Nauheim, Germany (5 Oct., 2015), oral presentation

Domestic conferences

1. M Somiya, and S Kuroda, Transfection efficiency of bio-nanocapsule-polyplex complex. 34th Annual Meeting of Molecular Biology Society of Japan, Yokohama, Japan (December, 2011), poster presentation
2. M Somiya, S Kuroda, Transfection Efficiency of Bio-nanocapsules-polyplex complex. The 34th Annual Meeting of the Molecular Biology Society of Japan, Kanagawa (December 2011), oral presentation
3. M Somiya, N Yoshimoto, and S Kuroda, Retargeting of polyplex by complexation with bio-nanocapsules. 28th Annual Meeting of Japanese Society of Drug Delivery System, Sapporo, Japan (July, 2012), oral presentation
4. M Somiya, S Kuroda, Analysis of The Cellular Uptake Mechanisms of Bio-nanocapsules-liposome Complex for Efficient Drug Delivery. Young Researcher's Conference of The Society for Biotechnology Japan, Miyazaki (July, 2013), poster presentation
5. M Somiya, S Kuroda, Development of Bio-nanocapsules-liposome Complex as a Nanocarriers Based on The Mechanisms of Cellular Uptake. 5th Young Researcher's Symposium of Division of Cell Processing Engineering, The Society for Biotechnology Japan, Miyazaki, Japan (July, 2013), oral presentation
6. M Somiya, K Yamaguchi, S Kuroda, Targeted delivery of siRNA into the cytoplasm of human hepatic cells by Bio-nanocapsule-liposome complex. Young Researcher's Conference of The Society for Biotechnology Japan, Kobe (July, 2014), poster presentation

7. M Somiya, S Kuroda, Elucidation of human hepatic cell-specific-cytoplasmic delivery of Bio-nanocapsule-liposome complex. The annual meeting of Central Japan Branch of the Society for Biotechnology, Japan (SBJ) at Nagoya, Japan (August, 2014), oral presentation
8. M Somiya, S Kuroda, Endocytosis-independent Cytoplasm-specific Delivery by Bio-nanocapsule-liposome Complex, 2014 Annual Meeting of The Society for Biotechnology Japan, Hokkaido (September, 2014), poster presentation
9. M Somiya, K Yamaguchi, S Kuroda, Application of the DDS Nanocarriers Possessing Infection Machinery of Hepatitis B Virus for Cancer Treatment. The 135th Annual Meeting of the Pharmaceutical Society of Japan, Kobe, Japan (March, 2015), invited lecture
10. M Somiya, Q Liu, S Kuroda. Elucidation of endosomal escape mechanisms of hepatitis B virus-inspired bio-nanocapsule-liposome complex. 31st Annual Meeting of Japanese Society of Drug Delivery System, Tokyo, Japan (July, 2015), oral presentation
11. M Somiya, K Shun'ichi, Intracellular trafficking and drug release of bio-nanocapsule-liposome complex, Young Researcher's Conference of The Society for Biotechnology Japan, Nagoya (July, 2015), poster presentation
12. M Somiya, K Yamaguchi, S Kuroda, Development of bio-nanocapsule-liposome complexes (virosomes) for the cytoplasmic siRNA delivery. 24th Drug Delivery Systems Conference, Shizuoka, Japan (4 Sep., 2015), oral presentation

Others: 7 presentations as co-presenter

Awards, grant, patent and outreach activity

Awards

1. Young Researcher's Award, Division of Cell Processing Engineering of The Society for Biotechnology, Japan (SBJ), 2013
2. Excellent Student Award of SBJ, 2013
3. Chair's Award, Central Japan Branch of SBJ, 2014
4. Annual Research Award of IGER (Integrative Graduate Education and Research) program, Nagoya University, 2014
5. IGER Annual meeting 2015 Poster Award, Nagoya University, 2015

Grant

1. Development of drug delivering nanocarriers derived from hepatitis B virus-like particle, achieving controlled intracellular fate. Grant-in-Aid for Japan Society for the Promotion of Science Fellows, 2013-2016

Patent

1. siRNA-encapsulated neutral or anionic liposomes and its preparation method. Japanese Patent Application No. 2014-170680

Outreach activity

1. Science cafe, speaker, Sanken Science Café, The Institute of Scientific and Industrial Research, Osaka University, 2 May, 2015

Acknowledgements

During this study, I received financial supports from Japan Society for the Promotion of Science (JSPS) as JSPS Research Fellow DC1, and Nagoya University Leading Graduate School Program (Integrative Graduate Education and Research (IGER) Program in Green Natural Sciences).

This study could not be accomplished without the aid of many people. First of all, I deeply appreciate to Prof. Shun'ichi Kuroda at Osaka University for his supervision throughout this study. Prof. Kuroda gave insightful comments and suggestions for this study. I would like to thank Prof. Andrés D Maturana for his scientific advices and warm encouragements. I would appreciate Profs. Hideo Nakano, Tsukasa Matsuda, and Tomoaki Niimi for their useful comments and supports during the thesis submission.

I also thank the member of Laboratory of Industrial Biosciences of Graduate School of Bioagricultural Sciences of Nagoya University, and Department of Biomolecular Science and Reaction of The Institute of Scientific and Industrial Research at Osaka University. Especially, Mr. Qiushi Liu, Ms. Kyoko Araki, and Ms. Kotomi Yamaguchi kindly contributed to this study. I was always helped and encouraged by the discussion with them. Furthermore, this study was done with supports from lots of colleagues and friends. I would sincerely express my thanks to all the people who participated in this study.

At the end of this thesis, I am grateful to my family, including parents, brother, sisters, and grandparents, for their patience, encouragement, and mental supports.